



Sessions

Session I -Diffraction Methods 1

S1 - 1

CHARACTERIZATION OF RETAINED AUSTENITE STABILITY IN MEDIUM MANGANESE DUPLEX STEELS BY HIGH ENERGY X-RAY DIFFRACTION AND DIC

M. Lamari^{1,2}, G. Geandier¹, K. Zhu², S. Allain¹

¹Université de Lorraine, CNRS, IJL, Nancy F-54000, France

²Arcelor Mittal, Maizières les Metz, France
guillaume.geandier@univ-lorraine.fr

Medium manganese steels belong to the family of steels with very high mechanical strength. Their good formability and high strength are due to their particular duplex microstructures that contain a micrometer-sized “ferritic” matrix and a significant amount of residual austenite that is transformed into martensite during mechanical loading. The progressive transformation of ductile austenite into hard martensite causes a rapid increase in macroscopic work hardening, due to the effect of transformation-induced plasticity. The understanding of the stability of residual austenite and the mechanical response of these steels is of great scientific and industrial interest.

Eight different microstructures have been designed via simple or double annealing, based on thermodynamical calculations in order to evaluate the respective effect of the morphology, composition and grains size on austenite stability. The formation of the duplex microstructures during intercritical annealing have been characterized in situ by high-energy X-ray diffractions (HEXRD) experiments on synchrotron beamline. Figure 1 presents a series of microstructure elaborated via simple annealing at different intercritical temperatures.

The tensile mechanical behaviour of the studied steels has been measured in combination with HEXRD experiments and Digital Image Correlation measurements. These unique in situ experiments permit to measure simultaneously the strain-induced martensitic transformation kinetics, the stress partitioning between phases (namely ferrite, austenite and martensite) using \sin^2 methods and the local strains all along the tensile specimens. These latter serve in particular to characterize Lüders and Portevin-Le Chatelier bands which affect the studied medium Mn

steels. Figures 2-4 present the evolution of Von Mises stresses in the main phases on four microstructures obtained by changing the intercritical temperature.

All those experimental inputs have served to develop an innovative mean field micromechanical framework to pre-

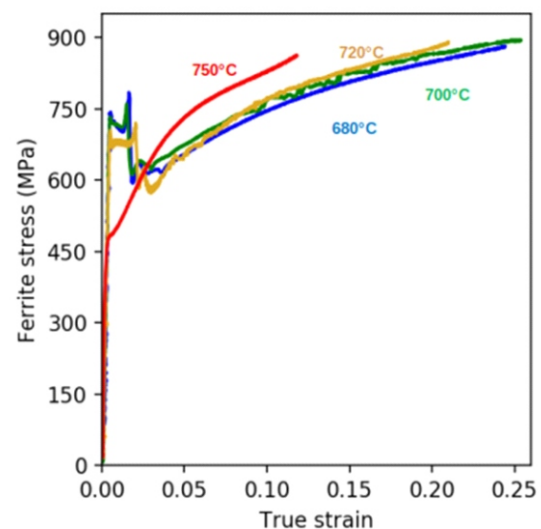


Figure 2: Comparison of Von Mises Stress in ferrite for four intercritical temperatures

dict the tensile behaviour of medium Mn steels with austenite-ferrite-martensite microstructures. It relies on the description of the local behaviours of each constituting phase

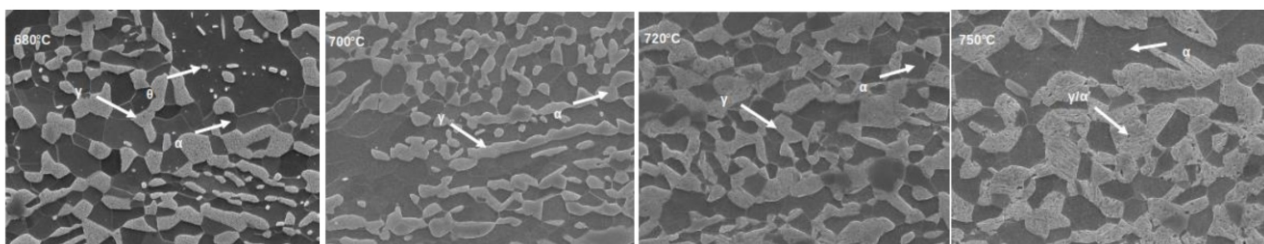


Figure 1: microstructure obtained after single annealing at four intercritical temperatures.

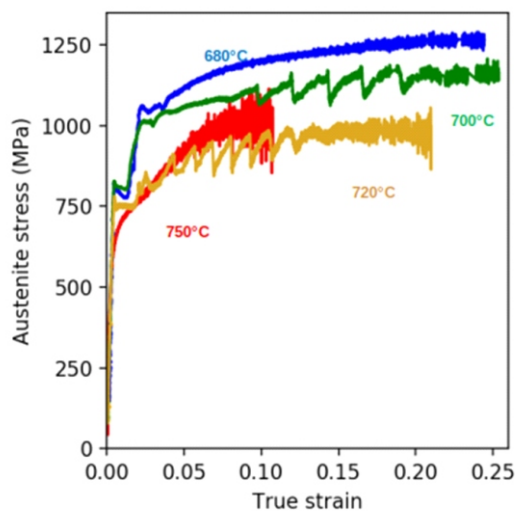


Figure 3. Comparison of Von Mises Stress in austenite for four intercritical temperatures.

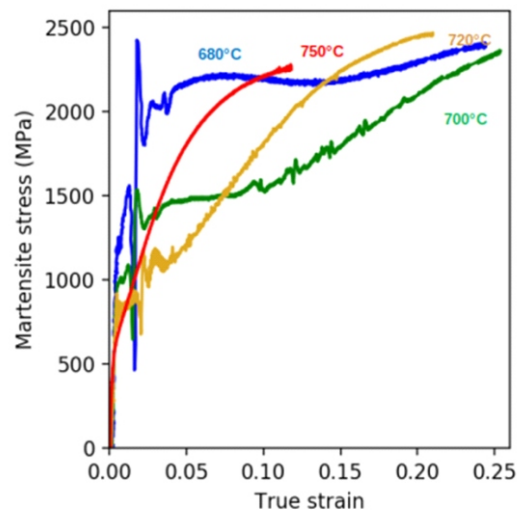


Figure 4. Comparison of Von Mises Stress in martensite for four intercritical temperatures,

and of the train-induced martensitic transformation of retained austenite, both calibrated on our HEXRD experiments [1].

1. Lamari, M. ; Allain, S.; Geandier, G.; Ponçot, M. ; Perlade, A. ; Zhu, K, International Journal of Plasticity , Vol. **173** (2024) 103866.

We acknowledge DESY (Hamburg, Germany), a member of the Hemholtz Association HGF, for the provision of experimental facilities. Parts of the research work was carried out at Petra III, P07 beamline. Beamtime was allocated for proposal 20191150 EC.



S1 - 2

A STUDY ON MINIMIZING MEASUREMENT TIME BASED ON ACTIVE EXPERIMENTATION FOR ENERGYDISPERSIVE X-RAY DIFFRACTION

Alexander Liehr^{1*}, Kristina Dingel², Daniel Kottke², Sebastian Degener³, David Meier^{2,4}, Bernhard Sick² and Thomas Niendorf¹

¹*Institute of Materials Engineering (University of Kassel), Mönchebergstr. 3, 34125 Kassel, Germany*

²*Institute of Intelligent Embedded Systems (University of Kassel), Wilhelmhöher Allee 7, 34121 Kassel, Germany*

³*Bundesanstalt für Materialforschung- und prüfung, Unter den Eichen 87, 12205 Berlin, Germany*

⁴*Helmholtz-Zentrum für Materialien und Energie, Hahn-Meitner-Platz 1, 14109 Berlin, Germany*
liehr@uni-kassel.de

Particularly in laboratory XRD measurements, where the intensities in diffraction experiments tend to be low, an adaption of the exposure time to the investigated microstructure is crucial [1]. Measurement times that are too short result in poor signal-to-background ratios or dominant signal noise, making subsequent evaluation more difficult or even impossible. Then, it is necessary to repeat measurements with adjusted, usually significantly longer measurement time. To prevent redundant measurements, it is state-of-the-art to use the full measurement range regardless of whether the measurement points are relevant and contribute to the subsequent materials characterization. Examples for such cases are texture [2] and residual stress measurements [3]. Since the first evaluation steps following the measurement are standardized procedures, they provide an interesting approach for intelligent methods directly embedded in the measurement sequence [4]. In the present study, different approaches are investigated that analyze the continuously growing data set during an energy dispersive diffraction measurement on a complex application like shown in [5]. Different selection strategies are proposed that intelligently choose the next point of investigation by means of key characteristics of prior acquired data. It is shown that such strategies are able to significantly minimize the required measurement time according to the material's microstructure without losing data quality for subsequent analyses, thus, open up the possibility for in process active experimental design.

1. T. Manns, B. Scholtes: Diffraction residual stress analysis in technical components — Status and prospects, *Thin Solid Films* (2012), doi:10.1016/j.tsf.2012.03.064.
2. D. Meier, R. Rangunathan, S. Degener, A. Liehr, M. Vollmer, T. Niendorf, B. Sick: Reconstruction of incomplete X-ray diffraction pole figures of oligocrystalline materials using deep learning. DOI: 10.1038/s41598-023-31580-1, *nature scientific Reports* volume 13, Article number: 5410 (2023).
3. B. Breidenstein, S. Heikebrügge, P. Schaumann, C. Dänekas: Influence of the Measurement Parameters on Depth-Resolved Residual Stress Measurements of Deep Rolled Construction Steel using Energy Dispersive X-ray Diffraction, *HTM, J. Heat Treatm. Mat.*, 75 (2020) 6, S. 419-432. DOI: 10.3139/105.110423.
4. K. Dingel, A. Liehr, M. Vogel, S. Degener, D. Meier, T. Niendorf, A. Ehresmann and B. Sick.: AI-Based On The Fly Design of Experiments in Physics and Engineering, *IEEE International Conference on Autonomic Computing and Self-Organizing Systems Companion (ACSOS-C)* (2021). <https://doi.org/10.1109/acsos-c52956.2021.00048>.
5. A. Liehr, T. Wegener, S. Degener, A. Bolender, N. Möller and T. Niendorf: Experimental Analysis of the Stability of Retained Austenite in a Low-Alloy 42CrSi Steel after Different Quenching and Partitioning Heat Treatments, *Adv. Eng. Mater.* 2023, DOI: 10.1002/adem.202300380.

S1-3

STUDY OF PLASTIC DEFORMATION IN TWO-PHASE CuZn39Pb3 BRASS ALLOY USING NEUTRON DIFFRACTION

A. Ludwik^{1*}, P. Kot², A. Baczański¹, M. Wroński¹ and Ch. Scheffzük³

¹AGH University of Krakow, Faculty of Physics and Applied Computer Science, al. Mickiewicza 30, 30-059 Krakow, Poland

²NOMATEN Centre of Excellence, National Centre for Nuclear Research, A. Sołtana 7, 05-400 Otwock-Świerk, Poland

³Karlsruhe Institute of Technology, Institute of Applied Geosciences, Adenauerring 20b, 76131 Karlsruhe, Germany
aludwik@agh.edu.pl

Brass alloys, due to their unique properties such as high thermal and electric conductivity, corrosion resistance and extraordinary antibacterial properties, have been widely used in industries such as electronics, automotive and sanitary industry [1]. Therefore, it is important to study plastic deformation of such materials at macroscopic scale, as well as at the scale of polycrystalline grains. Especially important is determination of the critical resolved shear stresses (CRSSs) necessary for activation of slip systems, as well as to measure the stresses at polycrystalline grains. In this work significantly textured two-phase CuZn39Pb3 brass was investigated and the mechanical behaviour of each phase of the brass was experimentally determined. The orientation distribution function for α and β phases, measured using X-ray diffraction, is shown in Fig. 1.

During the experiment carried out in this work, an increasing compressive stress was gradually applied to the sample and the evolution of the material was investigated, in particular the lattice strains in the polycrystal grains were measured by diffraction. The measurements were carried out *in situ* by using the time of flight (TOF) neutron diffraction to examine interplanar spacings (EPSILON diffractometer, JINR, Dubna).

Table 1. Experimental values of CRSS for slip system activated in the studied CuZn39Pb3 brass.

Phase	Slip system	CRSS (MPa)
(bcc)	{110} <111>	130
	{112} <111>	
(fcc)	{111} <110>	120

Based on the lattice strains determined by nine detectors having different orientations with respect to the sample, the crystallite group method (CGM) [2,3] was used to determine the stresses for selected grain orientations. It should be emphasised that different hkl reflections in both phases were measured for each direction of the scattering vector. Having measured stress tensor for chosen orientations of crystal lattice (Fig. 1) the evolution of the resolved shear stresses (RSS) for potentially active slip systems was found (Fig. 2). The experimental values of CRSS, given in Table 1, were determined as the values of significant change in the evolution of RSS during plastic deformation. The obtained CRSSs were then verified by elastic-plastic

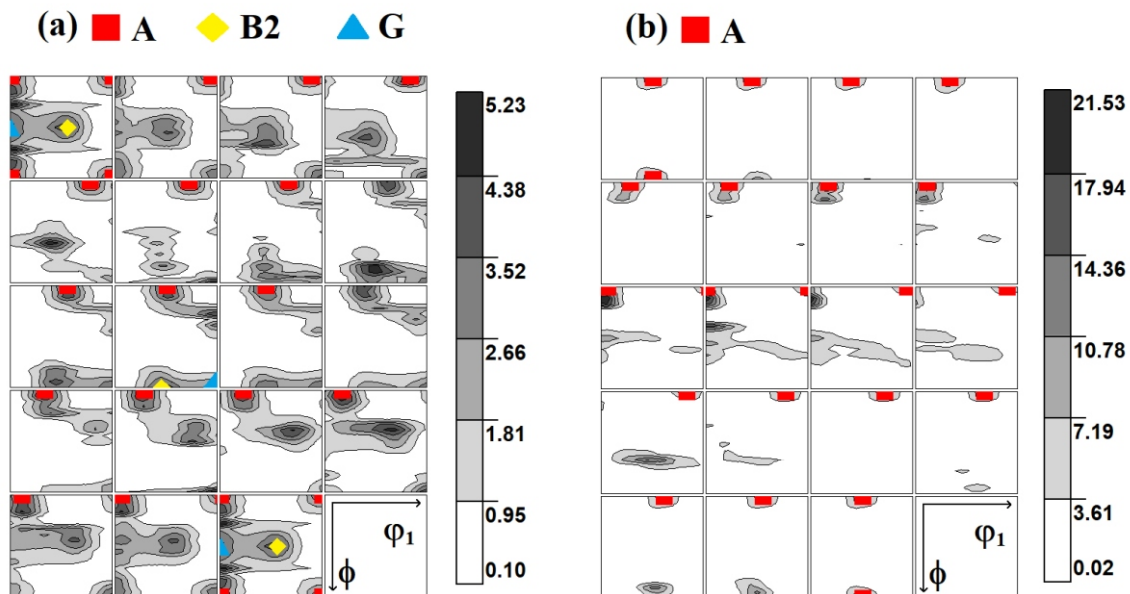


Figure 1. Orientation distribution function for the (a) and (b) phases of CuZn39Pb3 brass. Cross-sections through the reduced space of Euler angles are shown, with the step of 5° along the ϕ_2 axis.

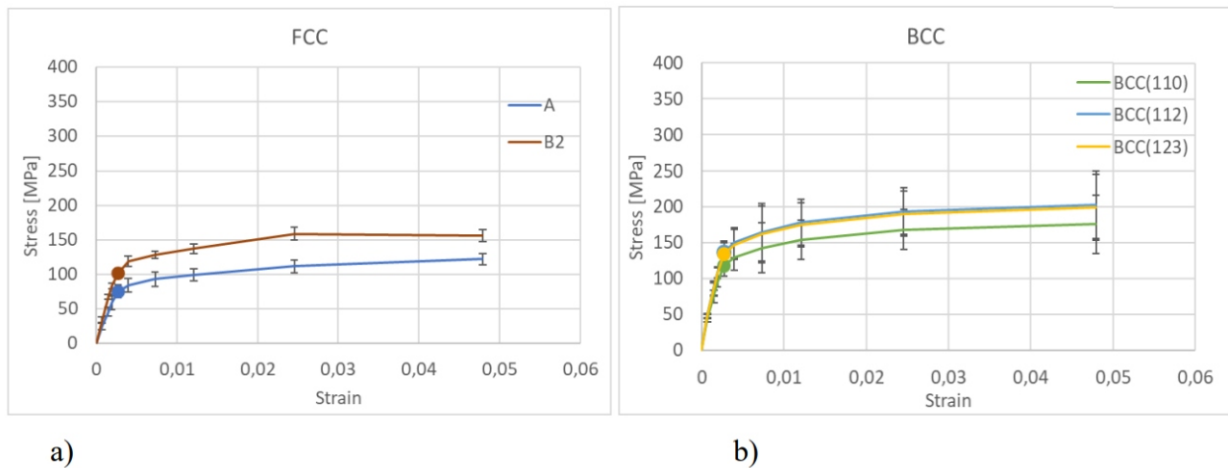


Figure 2. Resolved shear stress evolution during elastoplastic deformation versus sample strain E for slip systems in (a) and (b) phases of CuZn39Pb3 brass.

self-consistent (EPSC [4]) model obtaining a good agreement between measured and simulated evolutions of lattice strains, as well as macroscopic stress-strain curve.

It can be concluded that the values of different slip systems in both phases of studied brass are very similar.

1. P. Stavroulakis, A.I. Toulfatzis, G.A. Pantazopoulos, A.S. Paipetis, *Metals*, **12**, (2022), 246.
2. V. Hauk, *Structural and Residual Stress Analysis by Non-destructive Methods*, Amsterdam: ELSEVIER. 1997.

3. P. Kot, M. Wroński, A. Baczmański b, A. Ludwik, S. Wroński, K. Wierzbowski, Ch. Scheffzük, J. Pilch, G. Farkas, *Measurement*, **221**, (2023), 113469.
4. P. Lipinski, M. Berveiller, *Int. J. Plast.*, **5**, (1989), 149.

This work was financed by a grant from the National Science Centre, Poland (NCN), No. UMO-2023/49/B/ST11/00774. The research project was partly supported by the program "Excellence initiative – research university" for the AGH University of Science and Technology.

S1-4

DIFFRACTION STRESS MEASUREMENT IN SINGLE CRYSTALS

B. Ortner

*Retired from University Leoben, Leoben, Austria
Balder.Ortner@at*

Stress measurement using X-ray or neutron diffraction in single crystals can be described as a series of four different tasks.

- 1.) The exact orientation of the specimen is to be determined.
- 2.) One must find a sample of measureable lattice planes, which meets the demand for high accuracy of the result.
- 3.) Measure lattice plane distances.
- 4.) Calculate the stress tensor from these measured data.

For better understanding single crystal stress measurement it is helpful to compare it with stress measurement of a quasiisotropic polycrystalline material.

Ad 1: In a polycrystal there is of course no need to determine any orientation.

In single crystal measurement, however, it is indispensable to know the orientation. For orientation determination one can use either the Laue method or the aid of a texture goniometer.

Ad 2: For a measurement in a polycrystalline material the choice of the reflections (θ , hkl) is easy and well known: Bragg's angle must be as high as possible, the maximum value for the f values must be as large as possible,

and the distribution of θ over the orientation sphere and over $\sin^2 \psi$ must be as homogeneous as possible.

In a single crystal it is much more difficult since we usually cannot use only one (hkl) for the stress / strain measurement. That is, from a larger number of different (hkl)s, accessible for measurement, one must find a set which provides the highest accuracy. Accuracy of the then calculated stress tensor depends not only on the accuracy of the single measurements but also very much on the distribution of the (hkl)s [1, 2]. An extra difficulty in this search lies in the fact that each single $d(hkl)$ measurement has its own statistical error. This is due to different Bragg's angles θ .

Therefore it is virtually impossible to find the best set by hand selection, and we recommend the use of a computer programme.

Ad 3: Nearly all methods to measure polycrystals are designed so that only one type of (hkl) is used for all measurement points. (Best example is the \sin^2 method. [3]) This has the great advantage that a systematic error (for instance due to an improper alignment of the system) has virtually no detrimental influence to the resulting stress values. A poor alignment could only result in a wrong lattice parameter.

In single crystal stress measurement the situation is completely different. A bad alignment, say a wrong zero point of the goniometer, would always give the same error for θ , but therefore different systematic deviations in $d(hkl)$. And even very small errors in $d(hkl)$ would cause relevant errors in s_{ij} . The solution is not only to use (hkl) s with θ as high as possible but also to rely on one of the special methods for d -measurement in single crystals. This is the famous method developed by Bond [4], or, if one has no access to the needed Bond apparatus, the method proposed by the author [5]. Either method, properly applied, leads to the result of sufficiently accurate d -values.

Ad 4: Calculation of the stress (and strain) tensor is the easiest part of the whole endeavour: easy because the theory is very clear and not loaded with any uncertainties as in polycrystal measurement.

Two methods are available. In one method, developed by the author, one calculates at first the full strain tensor and then from it the stress tensor. The other method is based on the basic equation of diffraction stress measurement, the relationship among ϵ_{ij} and (θ, hkl) : the famous equation discovered by Dölle and Hauk. [6, 7]

We will demonstrate all these four steps in two examples: a single crystalline film with residual stress and one unstrained.

At first we will show how to determine the film's orientations by using a pole figure obtained in a texture goniometer.

After the orientation is known, all measureable reflections (hkl) together with their statistical accuracy are calculated.

Next we will show how a best set of (hkl) s is found. For that purpose we use a computer programme, the principle of it will be given.

Rather intricate is the actuation of the goniometer and the Eulerian cradle to get the specimen in the different positions where reflection can occur. Equations for the calculation of the Eulerian angles will be given.

Measurement of lattice plane distances is also somewhat complicated, be it using Bond's [4] or Ortner's [5] method. Since we do not have a Bond's apparatus we will only show how a measurement is done using Ortner's method. Rocking curves will be given and the method of how to optimise accuracy.

As already mentioned, the last step – the calculation of the stress tensor – is the easiest one, and it will be done using Dölle-Hauk's equation [6,7]. We will explain it with the aid of a system of linear equations.

1. B. Ortner, *Adv. X-ray Anal.*, **99** (1986), 113-118.
2. B. Ortner, *Met. Sci. Forum* **404-407** (2002) 323-328.
3. Victor Hauk Ed., *Structural and Residual Stress Analysis by Nondestructive Methods*: Elsevier 1989.
4. W.L. Bond, *Acta Cryst.* **13** (1960), 814-818.
5. B. Ortner, *J. Appl. Cryst.* **38**, (2005), 678-684.
6. H. Dölle, V. Hauk, *Z. Metallkde.* **70** (1979), 682-685.
7. H. Dölle, V. Hauk, *Z. Metallkde.* **69** (1978), 410-417.

S1 - 5

X-RAY MICRO- AND NANO-DIFFRACTION ANALYSIS OF RESIDUAL STRESSES IN THE COMPOUND LAYER AND DIFFUSION ZONE OF A GAS-NITRIDED STEEL

S.C. Bodner¹, M. Meindlhumer¹, J. Todt¹, K. Hlushko¹, S. Mirzaei^{2,3}, V. Strobl⁴,
B. Rübiger⁴, N. Schell⁵, M. Burghammer⁶, J. Keckes¹

¹Department Materials Science, Montanuniversität Leoben, A-8700 Leoben, Austria

²CEITEC BUT, Brno University of Technology, Purkynova 123, CZ-C61200, Czech Republic

³Fraunhofer Institute for Material and Beam Technology, D-01277 Dresden, Germany

⁴Rübiger GmbH & Co KG, Hardening Technology, 4600 Wels, Austria

⁵Helmholtz Zentrum Hereon, Outside station at DESY, D-22607 Hamburg, Germany

⁶European Synchrotron Research Facility ESRF, F-38043 Grenoble, France

sabine.bodner@unileoben.ac.at

Gas-nitriding is an industrially applied thermo-chemical surface modification process for steel to increase its hardness, wear resistance, and fatigue strength. A gradient material is created by the diffusion of nitrogen atoms in the base material, forming a ceramic compound layer on the surface. While the formation of the compound layer and its correlation with process parameters during gas-nitriding is well understood, challenges remain in fully elucidating spatially resolved values for its mechanical properties as well as the distribution of residual stresses in the near-surface region of steels. A detailed understanding of these characteristics is important as it will enable faster and more

accurate simulations, ultimately reducing the design effort for many industrial applications.

In this study, a gas-nitrided 42CrMo4 steel was investigated using correlative cross-sectional analyses to gain an in-depth understanding of the gradients in phase composition, microstructure, mechanical properties and distribution of residual stresses on the micro- and nanoscale. For this, the sample was investigated by cross-sectional micro- and nano-X-ray diffraction (CSmicroXRD and CSnanoXRD) in transmission geometry at ID13 beamline of the European Synchrotron Research Facility (ESRF) in Grenoble, France, and at the High-Energy-Materials-Sci-



ence beamline HEMS of the PETRAIII storage ring in Hamburg, Germany, using energies of 15.2 and 87.1 keV, respectively. Thus, a spatial resolution beyond 500 nm was achieved. The results from the synchrotron experiments were correlated with data from optical and scanning electron microscopy, microhardness profiling and nano-indentation. In addition, micromechanical cantilever bending tests were performed to evaluate stress-strain data and fracture toughness values in the compound layer.

CSmicroXRD analysis allowed the identification of a characteristic residual stress profile showing maximum compressive residual stresses of ~ 192 MPa at a depth of ~ 100 μm below the surface due to the (interstitial) diffusion of N atoms into the martensitic base material. The broadening of the observed hkl peaks as another consequence of the material's modification by N diffusion can be observed up to a depth of ~ 169 μm . This result is consistent with the results of (i) the chemical characterisation by energy dispersive X-ray spectroscopy and (ii) the microhardness profiling as the core hardness value of ~ 335 HV0.1 was determined at depths below the N diffusion zone.

Results of CSnanoXRD revealed that the tensile residual stresses were strong enough to crack the layer at the top

and further relax within the porous γ -nitride Fe_{2-3}N , which is ~ 3 μm thick. Below this, the compound layer consists mainly of the γ' -nitride phase (Fe_4N). This region of the compound layer comprises a further ~ 3 μm and is subjected to tensile stresses of ~ 500 MPa. The fact, that this tensile load relaxes at the interface between the γ' -nitride and the martensite base material by inducing tensile residual stresses in the martensite cannot be observed by any other characterisation methods than the one used, i.e. CSnanoXRD.

Micro-cantilever tests were performed on unnotched and notched beams in the γ' -nitride region. The results revealed a Young's modulus of $\sim 158 \pm 18$ GPa and a fracture toughness of $\sim 1.81 \pm 0.22$ $\text{MPa} \cdot \text{m}^{0.5}$. These results are lower than those obtained from nanoindentation experiments where the reduced Young's moduli for γ -nitride and γ' -nitride were determined to be 142 ± 6 and 201 ± 8 GPa, respectively.

Overall, this comprehensive analysis is an example of the use of advanced correlative characterisation in materials engineering applications, as the results provide a future perspective in the context of advanced characterisation of gradient materials.

Session II - Diffraction Methods 2

S2 -1

ROLE OF THE SECOND ORDER PLASTIC INCOMPATIBILITY STRESSES IN DEFORMED TITANIUM

S. Szostak¹, M. Wronski¹, S. Wronski¹, A. Baczanski¹, M. Marciszko-Wiackowska²

¹AGH University of Science and Technology, WFILS, al. A. Mickiewicza 30, 30-059 Kraków, Poland

²AGH University of Science and Technology, ACPIN, al. A. Mickiewicza 30, 30-059 Kraków, Poland
wronski@agh.edu.pl

One of the important reasons for the formation of residual stresses in polycrystalline materials is the anisotropy of the plastic deformation process. Different slip systems activity leads to different plastic deformations of polycrystalline grains. The resulting misfit (incompatibility) between neighboring grains is the source of the second order incompatibility stresses. These stresses cannot be measured directly but can be predicted by elastoplastic deformation models. They are correlated with the nonlinearity of lattice strains $\langle a \rangle_{\{hkl\}}$ vs. $\sin^2 \psi$ plots, determined experimentally [1].

The lattice strains $\langle a \rangle_{\{hkl\}}$ in plastically deformed material can be expressed as a superposition of strains induced by first order stresses and by second order incompatibility stresses which remain in a material (after unloading of the first order stress). It can be shown [2] that an average lattice parameter, measured in the direction of the scattering vector, can be expressed as:

$$\langle a \rangle_{\{hkl\}} = [F_{ij}(hkl, \psi)]_{ij} \frac{1}{q} \langle \sigma_{ij}^{II, model} \rangle_{hkl}] a_0 \quad (1)$$

where $F_{ij}(hkl, \psi)$ are diffraction elastic constants, σ_{ij} - macroscopic stresses, a_0 - the equivalent lattice parameter in a stress-free material. The $\sigma_{ij}^{II, model}$ tensor char-

acterises incompatibility stresses which remain after the unloading of macro-stresses ($\sigma_{ij} = 0$) and are caused by inter-grain plastic deformation incompatibility. The $\sigma_{ij}^{II, model}$ strain remains after unloading of the macrostresses and it can be calculated by the self-consistent model. The anisotropy of the incompatibility stresses can be correctly predicted by the model if the experimental texture is used as the input data. However, the absolute values of the stresses depend on the hardening process occurring during plastic deformation, which has generally a complicated character. Hence, to relate the magnitude of theoretical incompatibility stresses to the real one, an unknown scaling factor q is introduced. Only the amplitude of the theoretical function $\sigma_{ij}^{II, model}$ is rescaled by the q factor, while its dependence on the orientation of the scattering vector (i.e., on ψ and ϕ angles) is given by the model. It should be noted that if the determined value of q is near 1, the model predicts correctly the amplitude of the stress tensor, but if $q < 1$, the magnitude of theoretical stresses is overestimated.

In this work the stresses in deformed titanium alloys Ti40 are studied. The grazing incidence X-ray diffraction measurements [3] were performed during “*in situ*” tensile test in transvers direction. To predict the evolution of lattice parameter during tensile test the Elastic-Plastic Self-Consistent (EPSC) model developed by Lipiński and

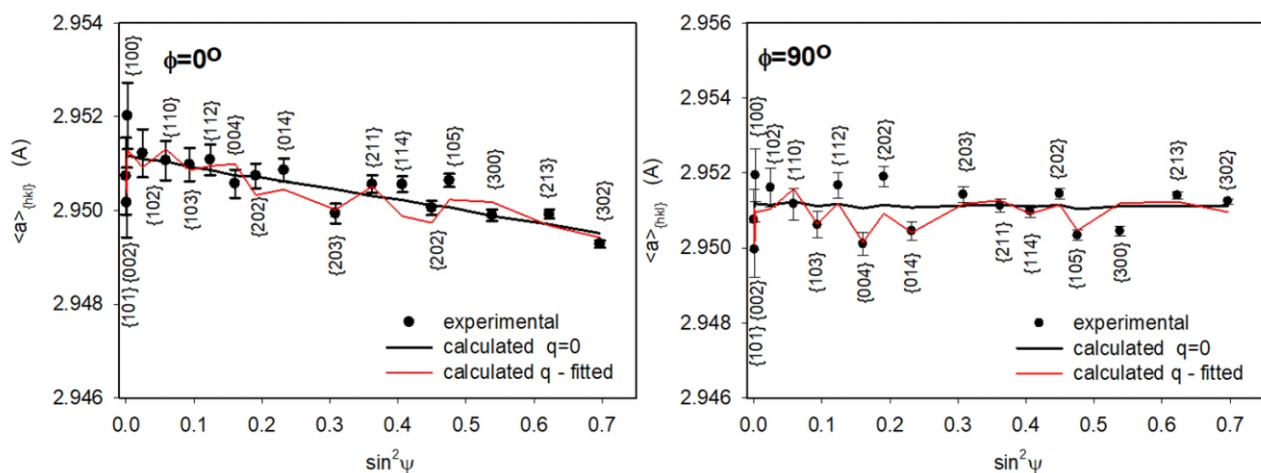


Figure 1. Measured lattice parameters (points) and theoretical results (lines) vs. $\sin^2 \psi$ for unloaded sample. Red lines for $q \neq 0$ (the second order stresses are taken into account) and black lines for $q=0$ (the influence of second-order stresses is neglected).

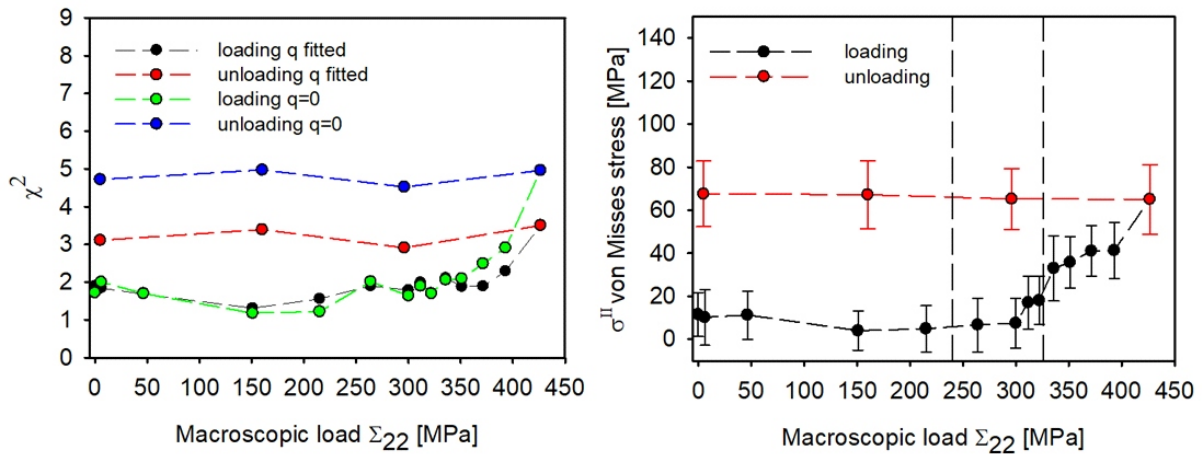


Figure 2. Evolution of fitting quality parameter χ^2 and mean von Mises second order stress $\sigma_{\text{Mis}}^{\text{II}}$ vs. macroscopic true stress Σ_{22} .

Berveiller [4]. The experimental $\langle a(\) \rangle_{\{hkl\}}$ vs. \sin^2 curve for unloaded sample was presented in Figure 1. As shown by red line, the quality of the fit improves significantly when the second order stresses are taken into account in the analysis and q is determined from Eq. (1). This important improvement of fitting quality – when the q parameter is adjusted – proves that the analysis is carried out correctly and the significant second order stresses are generated during plastic deformation in the studied sample.

In figure 2, the values of χ^2 parameter (characterising the quality of the least square fitting based on Eq. (1)) are compared for two different data treatments, assuming $q=0$ (the influence of the second-order stresses is neglected) or q is adjusted in Eq. 1. As seen, the value of χ^2 is much higher (worse quality of fitting) for the analysis with $q=0$ compared to that obtained when q is adjusted. The difference between χ^2 for two options of fitting is small in the case of elastic deformation, but it significantly increases with progress of plastic deformation, and remains large for

the unloaded sample. The mean value of von Mises stress $\sigma_{\text{Mis}}^{\text{II}}$ (mean value of $\sigma_{ij}^{\text{II}}(g)$, calculated over whole orientation space) increases when plastic deformation begins. It is also seen that the $\sigma_{\text{Mis}}^{\text{II}}$ value stay constant during sample unloading.

1. S. Wroński, A. Baczyński, R. Dakhloui, C. Braham, K. Wierzbowski and E.C. Oliver, *Acta Mater.* **55** (2007) 6219-6233 .
2. A. Baczyński, M. Wroński, P. Kot, S. Wroński, A. Łabaza, K. Wierzbowski, A. Ludwik, M. Marciszko-Wiąckowska, *Mater. Des.* **202** (2021) 109543.
3. S. Skrzypek, A. Baczyński, W. Ratuszek, E. Kusior, *J. Appl. Crystallogr.* **34** (2001) 427–435.
4. P. Lipinski, M. Berveiller, E. Reubrez, J. Morreale, *Arch. Appl. Mech.* **65** (1995) 291–311.

This work was supported by grants from the National Science Centre, Poland (NCN) No. 2019/35/O/ST5/02246.

RESIDUAL STRESS MEASUREMENT OF WELDED PIPE WITH SMALL BORE USING DOUBLE EXPOSURE METHOD

K. Suzuki¹, Y. Miura², H. Toyokawa³, A. Shiro⁴, S. Morooka⁵ and T. Shobu⁵

¹Niigata University, Nishi-ku, Niigata, 950-2181, Japan

²Central Research Institute of Electric Power Industry, Nagasaka, Yokosuka, 240-0196, Japan

³Japan Synchrotron Radiation Research Institute, Kouto, Sayo-cho, Hyogo, 679-5198, Japan

⁴National Institutes for Quantum and Radiological Science and Technology, Kouto, Sayo-cho, Hyogo, 679-5148, Japan

⁵Japan Atomic Energy Agency, Toukai-mura, Ibaraki, 319-1195, Japan
suzuki@ed.niigata-u.ac.jp

Recently stress corrosion cracking (SCC) of butt-welded stainless steel pipes with small bore have been found out. To solve this problem, it is necessary to create stress maps with high spatial resolution. However, it is difficult to measure stresses of welded parts due to coarse grains and dendrite structure.

A double exposure method (DEM) with high energy X-rays is useful for the stress measurement of welded parts [1-3]. In the DEM, a diffraction image from the transmission X-ray beam is measured at two positions P1 and P2 using an area detector (CdTe pixel detector) as shown in Fig. 1. The diffraction images of P1 and P2 are similar. Analyzing both images, we are able to determine each diffraction position, and calculate the diffraction angle, 2θ , from the diffraction radius $r (= r_2 - r_1)$ as $2\theta = 2 \arctan (r/L)$. In this method, the diffraction radius is determined by the relative difference between P1 and P2, so the error in the diffraction radius caused by the diffraction position within the sample can be cancelled out.

We prepared the austenitic stainless steel pipe with an outer diameter of 110 mm and a thickness of 11 mm (100A). These pipes were butt-welded by tungsten inert gas arc welding. A welded specimen for synchrotron experiments was removed from the welded pipe by electric discharge machining (EDM). The stress measurement of the welded specimen was performed at the BL14B1 of

SPRING-8. The X-ray energy was 70 keV, the dimensions of the X-ray beam were 0.4 mm^2 and the stress map was created by measuring the strains with a step of 0.4 mm .

In this study, the waves of P1 and P2 were obtained from a circumference integral of the diffraction images. The peak position was determined using cross-correlation algorithm between these waves [4]. As a result, we were able to efficiently determine the diffraction angles for all measurements. However, the hoop stress of the specimen has been released due to the removal with the EDM. To approximate the triaxial stress state, we consider the correction, assuming a plane strain. Applying the hoop stresses which are measured by the neutron method under a plane strain, the details of the stress maps in a triaxial stress state were obtained. Figure 2 shows the residual stress maps around the back-bead which is the welding bead on the inner surface. These stress maps support the phenomenon that the SCC occurs from the boundary with the heat affected zone of the inner surface of the butt-welded pipe.

1. K. Suzuki, T. Shobu, A. Shiro, *Materials Research Proceedings*, **6**, (2018), pp. 69-74.
2. K. Suzuki Y. Miura, A. Shiro, H. Toyokawa, C. Saji, S. Morooka, T. Shobu, *Key Engineering Materials*, **968**, (2023), pp. 3-8.

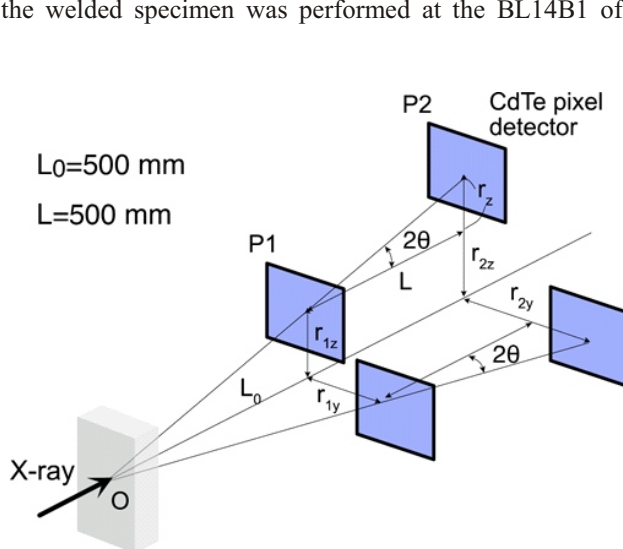


Figure 1. Double exposure method. The diffraction is measured by the area detector at P1 and P2.

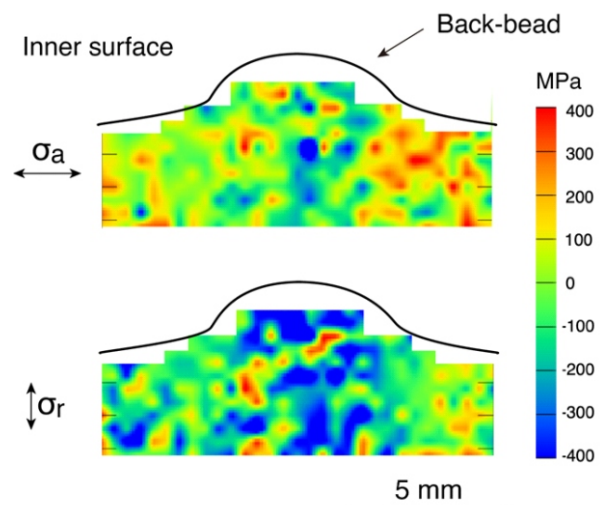


Figure 2. Residual stress maps around back-bead of welded pipe. The axial and radial stresses are obtained by combining the axial and radial strains measured by the DEM and the hoop stress measured by neutrons.



3. Y. Miura, K. Suzuki, S. Morooka, T. Shobu, *Quantum Beam Science*, **8**, (2024), 1.
4. K. Suzuki and Y. Miura, *J. Materials Science, Japan*, **72-4**, (2024). To be published.

This work was supported by JSPS KAKENHI No. 22K03819. The synchrotron radiation experiments were

performed at the QST beam-line BL14B1 with the approval of QST (No. 2023A3684) and QST-ARIM (JPMXP1223 QS0011). The neutron experiments were carried out under the Inter-University Program for the Joint-use of JAEA/QST Facilities, Nuclear Professional School, School of Engineering, the University of Tokyo, at the Research Reactor JRR-3, JAEA (No. 2023105204).

S2 - 3

IN-SITU DIFFRACTION ANALYSIS OF ELASTIC-PLASTIC BEHAVIOUR OF DP1000

J. Rebelo Kornmeier¹, S. Vizthum², M. Hofmann¹, M. Gruber², R. Norz², E. Maawad³, J. Mendiguren⁴, W. Volk²

¹Heinz Maier-Leibnitz Zentrum (MLZ), Technical University of Munich, Garching, Munich, Germany

²Chair of Metal Forming and Casting, Technical University of Munich, Garching, Munich, Germany

³Helmholtz-Zentrum Hereon, Institute of Materials Physics, Geesthacht, Germany

⁴Mondragon Unibertsitatea, Faculty of Engineering, Mech. and Ind. Production, Mondragon, Gipuzkoa, Spain
Joana.kornmeier@frm2.tum.de

Due to the significant elastic nonlinearity and strain dependence, modelling the elastic behaviour of dual-phase steels is still a challenge. Microscopic in-situ studies are required since it is anticipated that the origins of this can be traced back to microstructural behaviour. However, analysis is difficult as the martensite and ferrite diffraction peaks overlap. In this study, we examined the steel CR590Y980T (DP1000) in a continuous cyclic tension-compression test while exposed to synchrotron radiation at DESY's Petra III High Energy Material Science. An assessment method to examine the dual-phase diffraction profiles in order to differentiate martensite and ferrite is demonstrated. The respective phase fraction, were corroborated by scanning electron microscopy (SEM) analysis. The findings contrib-

ute to a better understanding of the microstructure-level elastic-plastic behaviour of DP steels and hold tremendous promise for characterisation and modelling improvements related to springback prediction.

The difficulties in simulating the behaviour of elastic materials can be summed up as follows: determination of the initial elastic modulus; the onset of plastic yielding in the case of a steady elastic-plastic transition; early re-yielding or a significant Bauschinger effect. The methodology of Li and Wagoner [1], who equated anelasticity to nonlinear elasticity in their thorough investigation, is used in this work. Figure 1 shows a graphical and mathematical description of that [2].

In the current study, continuous cyclic tensile tests are carried out. High frequency (1 Hz) diffraction measurements are synchronous performed with these tests. Additionally, during the test, the specimen temperature is recorded for analysis and determination of the loading modulus and the onset of plastic yielding via the thermoelastic effect [3]. Furthermore, a continuous tension-compression test is performed to examine the microstructural behaviour both for the unloading and for compression. In this way, early re yielding, or the Bauschinger effect is analyzed.

In the present study, it was possible to assess ferrite and martensite individually using a diffraction profile evaluation method which was capable to extract both martensite as well as ferrite peak information. Form these results, interphase stresses were calculated and directly compared to the macroscopic material behaviour. As an example the results for the (211) lattice plane are shown in Figure 2 and 3.

It turned out that when the specimen is elastically released, the martensite absorbs much greater stresses and restricts the ferrite phase to compression. A relation between the behaviour of elastic strain and the residual micor-stresses of the second order could be established. The microstructural evaluation from the tension-compression tests was further used to analyse the re-yielding behaviour and microscopically show the Bauschinger effect. In addition, the phase interaction, which enables the material

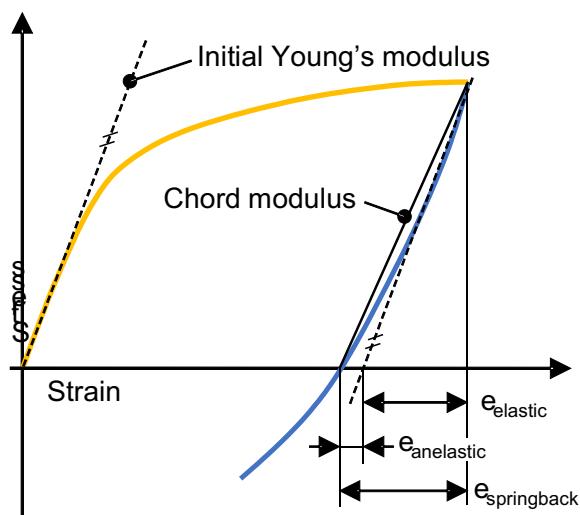


Figure 1 Schematic stress-strain curve to illustrate material behaviour and parameters.

$$\text{springback} \quad \text{anelastic} \quad \text{elastic} \quad \text{anelastic} \quad \overline{E_0} \quad (1)$$

E_0 is the initial Young's, the current true stress or Cauchy stress

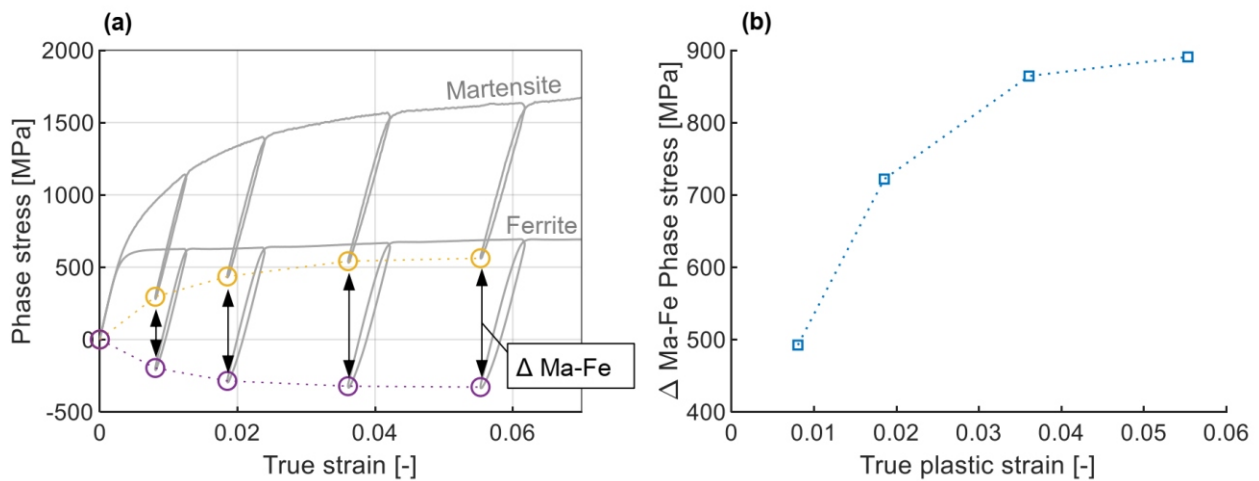


Figure 2. (a) Phase stress versus true strain. Highlighted are the phase stress at unloaded state (0 MPa) and their difference (Δ). (b) Delta values at unloaded state versus true plastic strain.

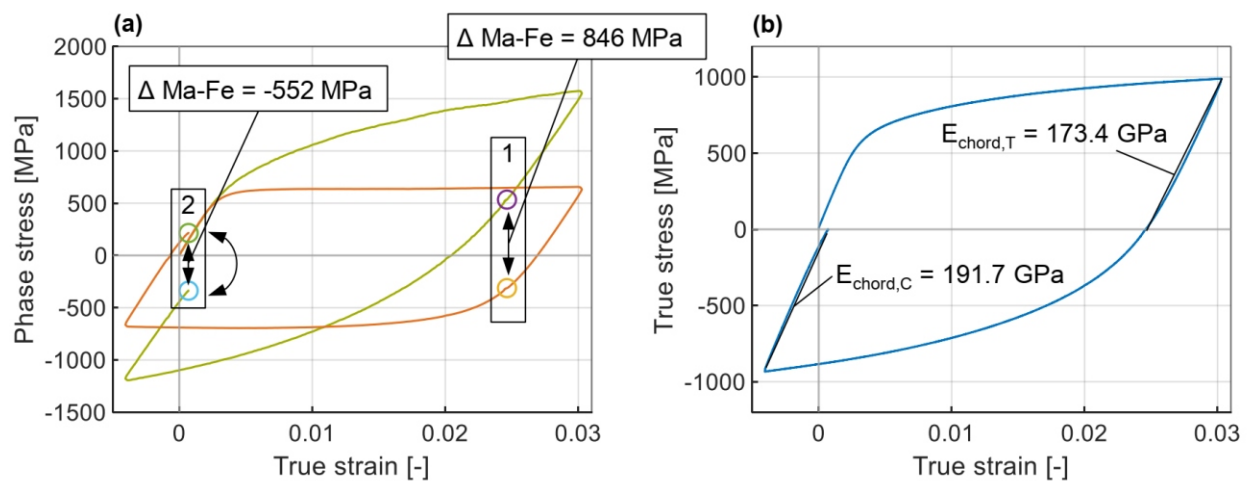


Figure 3. (a) Phase stresses and the interphase stresses at zero macroscopic stress after tensile loading (state 1) and after compressive loading (state 2) are plotted. (b) True stress-strain curve and elastic chord moduli for tension $E_{\text{chord,T}}$ and compression $E_{\text{chord,C}}$

to recover during variations in load was demonstrated. After compressive loading, the phase stresses in this process caused a rise in the macroscopic elastic modulus.

1. D. Li and R. H. Wagoner, *Acta Mater.*, **206**, (2021), 116625.
2. Z. Arechabaleta, Peter van Liempt, J. Sietsma, *Acta Mater.*, **115**, (2016), pp. 314–323.
3. S. Vitzthum, J. Rebelo Kornmeier, M. Hofmann, M. Gruber, E. Maawad, A. C. Batista, C. Hartmann, W. Volk, *Materials & Design*, **162**, (2022), 110753.



S2 - 4

INVESTIGATION OF THE EFFECT OF LASER SHOCK PEENING ON THE FATIGUE RESISTANCE OF RIVETED LAP JOINTS OF AEROSPACE GRADE 7XXX SERIES ALUMINUM

Ogün Baris Tapar¹, Jérémy Epp^{1,2}

¹Leibniz Institute for Materials Engineering, Badgasteiner Str. 3, 28359 Bremen, Germany

²MAPEX Centre for Materials and Processes, University of Bremen, Badgasteiner Str. 3, 28359 Bremen, Germany

tapar@iwt-bremen.de

Different joining techniques are widely used in aircraft structure. Due to dominant advantages in many aspects including stability, high reliability, simple production process and low cost, riveting is widely used. Riveted lap joint structure includes two overlapping plates connected with rivets. As weakest structures in modern aircraft assembly, these joints are prone to fatigue failures due to the load cycles in service. Stresses resulting from tensile loading superimpose with the stress caused by a phenomenon called secondary bending, leading to complex loading scenario.

Extensive studies have been conducted in the past to investigate the relation between fatigue life and several effecting factors such as rivet design, rivet material, and manufacture routine. Most of investigation ascribed to the generation of residual stresses in the sheet material as a primary reason of fatigue life enhancement. These findings shift the focus of the recent studies on additional processes that generates beneficial residual stresses. In this manner, one of the highly used techniques to increase fatigue life of rivet holes is split-sleeve cold expansion in which a tapered mandrel covered by an internally lubricated split sleeve is pulled through the hole to create a plastically deformed area, generating beneficial compression residual stresses around the rivet hole.

Despite widely reported positive effect of cold expansion on the fatigue life of riveted joints, cold expansion also exhibits inherent disadvantages. In particular, non-homogeneous residual stresses are generated in axial and hoop direction and tensile residual stresses could result in critical

regions. As well, considerable surface deformation especially on the mandrel outlet side of the hole takes place where the highest compressive residual stresses results, but also enhances the level of tension in the transition zone at some distance away from the hole which therefore could act as crack initiation points. Laser shock peening has been considered for the treatment of critical regions of riveted lap joints, since it offers certain flexibility and possibly a beneficial distribution of compressive residual stresses.

The aim of this study is to evaluate the effect of laser shock peening on the fatigue life of riveted lap joint structure compared to conventional treatment using cold expansion. To reach the given aim, LSP parameter study was performed to evaluate the process impact on residual stress distribution and surface topography. Riveted lap joint samples were treated with different parameters and evaluated regarding their fatigue properties. Different performances of the LSP treated samples could be observed, compared to the samples treated with cold expansion, with partly higher and partly lower fatigue life. Comprehensive analysis of the underlying mechanisms was analysed by investigating the stability of generated the residual stresses at different number of cycles by using non-destructive energy dispersive synchrotron measurements at DESY. Additional analysis of fatigue crack initiation and propagation, as well as local loading strain analysis allowed identifying critical regions and enabled to correlate the local loading condition with the observed behaviour of the treated parts.

SYNCHROTRON DIFFRACTION: A SUITABLE TOOL FOR RESIDUAL STRESS ANALYSIS IN A Ni-BASED WELDED PLATE

D. Canelo-Yubero¹, P. Staron¹, G. Abreu Faria¹, R. Badyka²

¹Helmholtz-Zentrum Hereon, Max-Planck-Str. 1, 21502 Geesthacht, Germany

²Électricité de France Lab les Renardières, F-77818 Moret sur Loing, France
David.canelo@hereon.de

Unintentional residual stresses within a component can strongly affect its structural integrity and therefore reduce its service life. This is the case for welded structures, in which the material misfit arising from the thermal and external load applied during welding generates stresses that can overcome the yield stress of the materials. Therefore, it is common to apply subsequent thermal treatments to relieve or at least partially relax these stresses.

Nickel alloys are used, among other fields, in welded components for pressurized water reactors (PWRs). Nickel alloy dissimilar metal welds in PWRs are not heat treated, leading to the presence of large residual stresses which originate higher susceptibility to stress corrosion cracking, fatigue, and creep. Many efforts have been performed so far to understand the development of these residual stresses (e.g. the European Network on Neutron Techniques Standardization for Structural Integrity - NeT [1]). Measurements and simulations have been part of these efforts, with the former usually evaluated using the neutron diffraction technique. Its large scattering angles and gauge volume (compared to synchrotron diffraction) allows to determine the strain in three orthogonal directions deep inside the bulk of the welded material even when the dimensions of the plate are centimetres or the grain size is large.

A nickel-based alloy plate (Alloy 600) with a 3-pass slot weld (named TG6 hereafter) was produced using an automated gas tungsten inert gas weld (GTAW/TIG) with a compatible nickel-based Alloy 82 filler material [2]. The dimensions of the plate are $150 \times 200 \times 12 \text{ mm}^3$ with a weld bead dimension equal to $76 \times 5 \times 5 \text{ mm}^3$. An automated TIG welding machine has been employed for welding the plates at the Électricité de France (EDF) laboratory in Chatou, France. The main microstructural features, detailed in [2], are: 1) the grain size in the zones unaffected by welding is approximately $20 \text{ }\mu\text{m}$; 2) grain coarsening starts at around $\sim 1 \text{ mm}$ away from the fusion boundary of the weld to parent material; 3) the coarsest grain size in the heat affected zone of the weld is equal to $40 \text{ }\mu\text{m}$ and within the weld, the grain size increases to $200 \text{ }\mu\text{m}$ in the first weld bead; 4) a weak rolling texture in longitudinal direction for parent material and also a strong texture in the normal direction on top weld measurement have been documented. However, at the bottom of the weld, the orientation density is low in longitudinal direction. Neutron diffraction has al-

ready been employed to capture the residual stress within the bulk of this sample at different positions [2].

The use of synchrotron diffraction is initially hindered for the strain calculation in the direction orthogonal to the baseplate as it would lead to a high path length for the beam, owing to the low scattering angle. Nevertheless, synchrotron diffraction can be advantageous if some conditions are fulfilled: a) the absence of stresses orthogonally to the plate, b) the sample can be oscillated to increase the statistics in the welded and heat affected zones, and c) the use of the \sin^2 method. The first requirement was proven in [2], the second can be overcome with a specific setup, and the latter can be easily implemented with a synchrotron measurement.

Different techniques can be used at a synchrotron facility to determine bulk residual stresses. A monochromatic X-ray beam with high photon energies in combination with a conical slit cell (CSC) [3] enables the determination of the strain components over the whole sample thickness with sufficient spatial resolution. A white X-ray beam in transmission mode also enables strain measurements within the bulk of the part while the reflection mode allows the characterization of residual stresses close to the surface.

With the aim of strengthening the industrial access to the non-destructive synchrotron technologies at large-scale facilities, the EU project EASI-STRESS is using the TG6 sample for the benchmarking and cross-comparison between different facilities. With this work, we aim at showing that synchrotron diffraction can be a suitable tool for the measurement of residual stresses in a Nickel-based welded plate. The P07/HEMS and P61A/WINE beamlines at DESY, operated by Hereon, were used for this purpose. Different scan lines in transverse and longitudinal directions were studied at different depths from the top surface. Moreover, the possible presence of shear stresses will be addressed.

1. <https://www.net-network.eu/>
2. V. Akrivos, R.C. Wimpory, M. Hofmann, B. Stewart, O. Muransky, M.C. Smith, J. Bouchard, *J. Appl. Crystallogr.* **53**, (2020), 1181.
3. P. Staron, T. Fischer, J. Keckes, S. Schratte, T. Hatzenbichler, N. Schell, M. Müller, A. Schreyer, *Mater. Sci. Forum*, **768-769**, (2014), 72.



S2 - 6

PROBING DEFORMATION BEHAVIOR OF A REFRACTORY HIGH-ENTROPY ALLOY USING *IN SITU* NEUTRON DIFFRACTION

Wenli Song^{1,2}, Yuanbo Zhou^{1,2,3,4}, Fei Zhang¹, Yanchun Zhao³, Dong Ma⁴

¹Institute of High Energy Physics, Chinese Academy of Sciences, Beijing 100049, China

²Spallation Neutron Source Science Center, Dongguan 523803, China

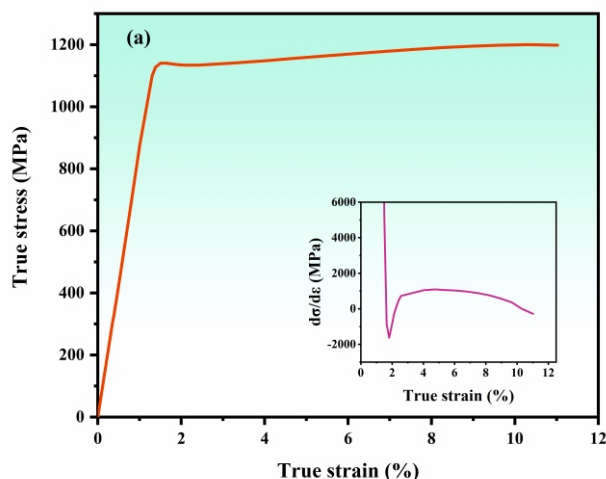
³State Key Laboratory of Advanced Processing and Recycling of Non-Ferrous Metals, Lanzhou University of Technology, Lanzhou 730050, China

⁴Neutron Science Center, Songshan Lake Materials Laboratory, Dongguan 523808, China
songwl@ihep.ac.cn, zhaoyanchun@lut.edu.cn, dongma@sslslab.org.cz

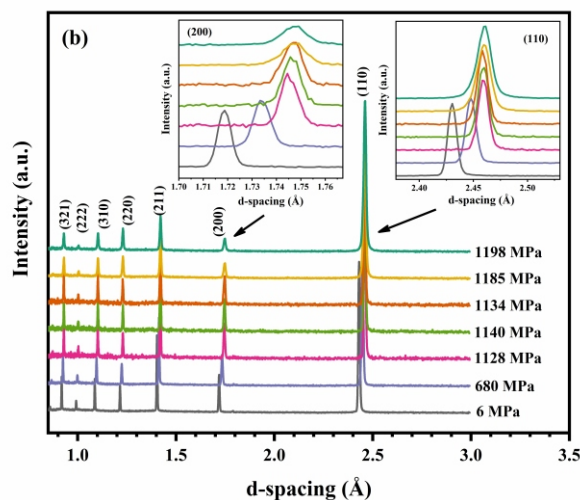
The grain orientation-dependent lattice strain evolution of a $(\text{TiZrHfNb})_{98}\text{N}_2$ refractory high-entropy alloy (HEA) during tensile loading has been investigated using in situ neutron diffraction. The equivalent strain-hardening rate of each of the primary $\langle hkl \rangle$ -oriented grain families was found to be relatively low, manifesting the macroscopically weak work-hardening ability of such a body-centered cubic (BCC)-structured HEA. This finding, along with the post-mortem transmission electron microscopy (TEM) characterization, is indicative of a dislocation planar slip mode that is confined in a few single-slip planes and leads to in-plane softening by high pile-up stresses. In particular, during plastic deformation, the $\langle 110 \rangle$ -oriented grains yield preferentially, followed by lattice relaxation, while the load transfers to the $\langle 200 \rangle$ -oriented grains as a result of plastic anisotropy. Our work provides a new perspective for understanding the strain-hardening behaviour and the role of planar slip in the plastic deformation of BCC-structured HEAs.

1. Z. F. Lei, X. J. Liu, Y. Wu, H. Wang, S. H. Jiang, S. D. Wang, X. D. Hui, Y. D. Wu, B. Gault, P. Kontis, D. Raabe, L. Gu, Q. H. Zhang, H. W. Chen, H. T. Wang, J. B. Liu, K. An, Q. S. Zeng, T. G. Nieh, Z. P. Lu, *Nature*, 563, (2019), 546.
2. Y. Wu, W. H. Liu, X. L. Wang, D. Ma, A. D. Stoica, T. G. Nieh, Z. B. He, Z. P. Lu, *Appl. Phys. Lett.*, 104, (2014), 051910.
3. M. Naeem, H. Y. He, F. Zhang, H. L. Huang, S. Harjo, T. Kawasaki, B. Wang, S. Lan, Z. D. Wu, F. Wang, Y. Wu, Z. P. Lu, Z. W. Zhang, C. T. Liu, X. L. Wang, *Sci. Adv.*, 6, (2020), eaax4002.

This work was supported by the financial support from the National Key R&D Program of China (No. 2020YFA 0405902), the Mobility Programme endorsed by the Joint Committee of the Sino-German Center (M-0728) and the invitation from Forschungs-Neutronenquelle Heinz Maier-Leibnitz (FRM II). The neutron diffraction experiments at the Materials and Life Science Experimental Facility of the J-PARC were performed under a general user program (Project No. 2020A0241).



a)



b)

Figure 1. (a) True tensile stress-strain curve for tensile loading of the $(\text{TiZrHfNb})_{98}\text{N}_2$ RHEA, the inset in (a) shows the work-hardening rate curve of the current RHEA. (b) Selected neutron diffraction patterns collected with respect to the loading direction during tensile loading of $(\text{TiZrHfNb})_{98}\text{N}_2$ RHEA.

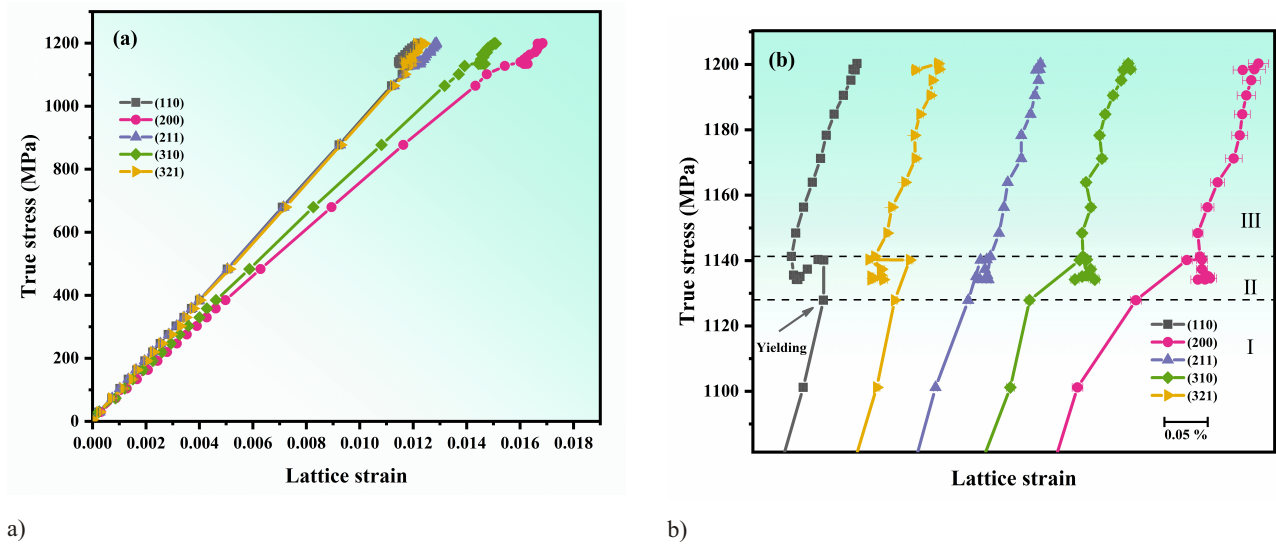


Figure 2. (a) True stress–lattice strain curves for five $\langle hkl \rangle$ //LD families of grains obtained during tensile loading at room temperature. (b) Magnified lattice strain evolution with true stress for the $(\text{TiZrHfNb})_{98}\text{N}_2$ RHEA during yield and plastic deformation process.

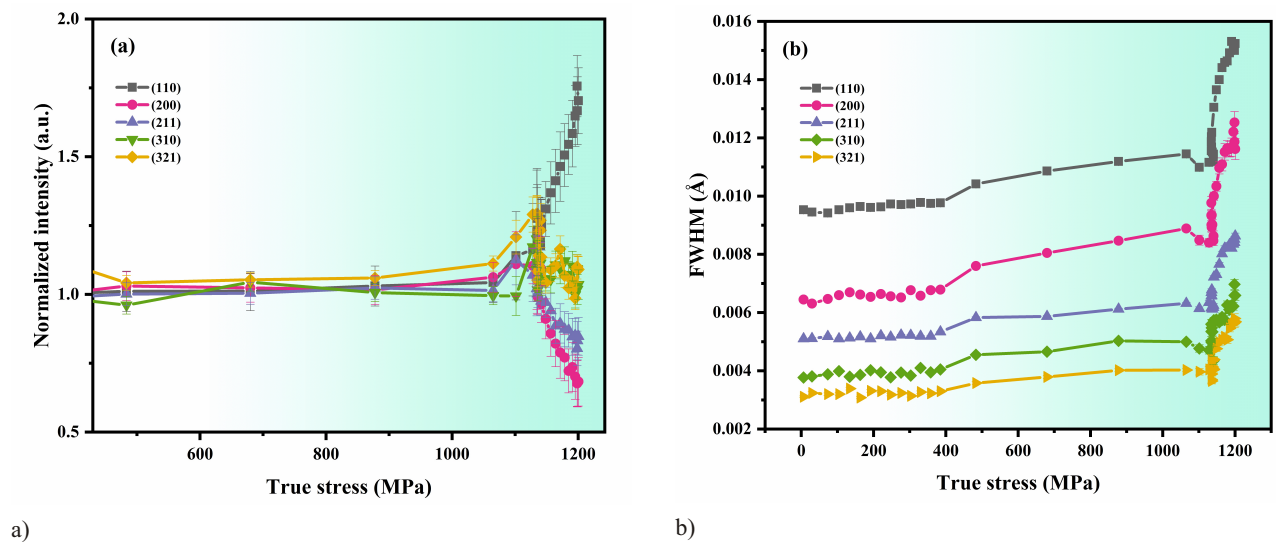


Figure 3. Evolution of diffraction peak intensity (a) and FWHM (b) of the $(\text{TiZrHfNb})_{98}\text{N}_2$ RHEA as a function of applied stress during tension.



Session III - Mechanical Relaxation Methods 1

S3 - 1

EXPERIMENTAL VALIDATION OF IHD CALIBRATION COEFFICIENTS DETERMINED BY MACHINE LEARNING FOR LAYERED COMPOSITE MATERIALS

T.C. Smit¹, S. Lee², R.G. Reid¹, D. Kim²

¹*School of Mechanical, Industrial and Aeronautical Engineering, University of the Witwatersrand, Private Bag 3, Wits 2050, South Africa*

²*Department of Mechanical Engineering, Seoul National University, 1 Gwanak-ro, Gwanak-gu, Seoul 08826, Korea
Teubes.Smit@wits.ac.za*

Incremental hole-drilling (IHD) is a popular relaxation technique for residual stress measurement. It consists of incrementally drilling a small hole into a sample, thereby removing stressed material, while measuring the accompanying deformations on the top surface for each incremental depth, commonly using a strain gauge rosette that is concentric with the hole. Calibration coefficients are required to relate the measured deformation to the residual stress distribution that existed in the material prior to drilling. The ASTM E837 standard [1] provides polynomial functions for determination of the necessary calibration coefficients for the integral computational method in metallic materials for any combination of hole diameter, specimen thickness, material properties and incremental depth distribution. However, in the case of layered composite materials, the calibration coefficients must be determined from finite element (FE) analyses [2] for the specific combination of hole diameter, sample thickness, material properties and stacking sequence of the sample being investigated. Hundreds of additional FE analyses may be required for a single laminate configuration, depending on the uncertainty sources considered, which can become strenuous if numerous laminate configurations are under investigation.

This work investigates the use of machine learning (ML) to predict calibration coefficients of the integral method for every possible symmetric and balanced config-

uration of an eight-ply fibre reinforced plastic (FRP) laminate where the plies can be orientated at 0°, 90° or ±45°. The architecture of the ML model is primarily grounded in operator learning, specifically Deep Operator Network (DeepONet) [3]. This architecture was modified by integrating a linear branch network with a graph convolution trunk network, enabling the effective learning of data from FE analyses. The model is trained using the displacement field on the top surface of the sample for every stress application depth and drilling increment for 30 out of the 70 possible symmetrical and balanced eight-ply laminate configurations. Laminates selected for experimental comparison were excluded from the training set. In the training of the model, a combined mean squared error loss for displacement and strain was utilized while stress error served as the metric for validation in each training epoch. Upon completion of the training, the model is capable of constructing a calibration matrix through forward predictions of unit stress. The error in the predicted calibration coefficients, resulting from the prediction of configurations outside the training data (epistemic uncertainty), was estimated using Monte Carlo dropout, a technique that approximates a Gaussian process.

IHD was performed using a SINT MTS3000-Restan system to drill a hole of 1.54 mm diameter in FRP laminates of [0/0/90/90]_s and [0/+45/90/-45]_s construction and

Table 1. Sources of uncertainty and their assigned probability density functions.

x_i	Description	$p(x_i)$	Type	Nominal value, uncertainty
h_0	Zero depth	Rectangular	B	0 m, 13.33 m
h_i	Incremental depths	Rectangular	B	13.33 m, 0.50 m
$meas$	Measured experimental strain	Normal	B	Indicated strain, 1.54%
$noise$	Experimental noise	Normal	A	0, 0.61 m/m
FE	Finite element calculations	Normal	B	FE output, 2%
ML	Machine learning predictions	Normal	A	ML output, Monte Carlo dropout

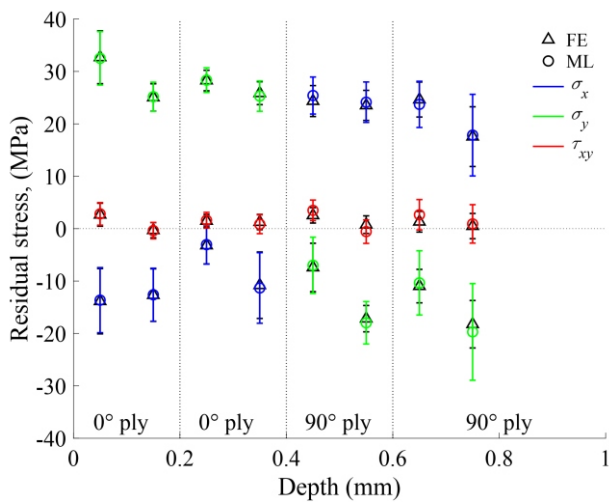


Figure 1. Measured residual stress distribution in a $[0/0/90/90]_s$ laminate.

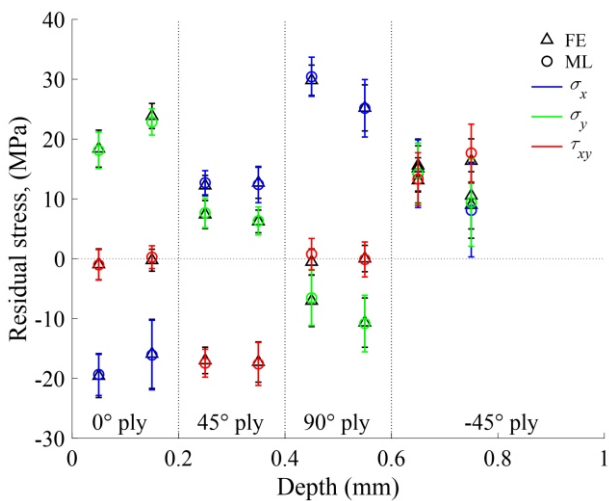


Figure 2. Measured residual stress distribution in a $[0/45/90/-45]_s$ laminate.

a thickness of 1.6 mm manufactured from E-glass/epoxy prepreg material. Sixty depth increments were performed up to the midplane to minimize drilling induced heating ef-

fects and to obtain sufficient strain data for robust interpolation to eight computational depth increments, including associated zero depth and incremental depth uncertainties. The dominant experimental and computational uncertainty sources considered are provided in Table 1. The calculated residual stress distributions obtained through the use of FE generated calibration coefficients and ML predicted calibration coefficients are presented in Figs. 1 and 2.

The agreement in calculated stress distributions demonstrates that calibration coefficients predicted by ML have practically acceptable accuracy while significantly reducing the number of FE analyses required. While this is perhaps not fully appreciable when dealing with eight plies and 70 possible configurations, it demonstrates the possible implementation when dealing with 16 plies and thousands of possible configurations, for example. It also demonstrates the feasibility of creating a much larger database and ML model for the residual stress community that can include ranges for any combination of material properties, number of plies, ply thickness and hole diameter. This could allow rapid generation of calibration coefficients for any combination of laminate configuration, material properties and hole diameter without the need to perform any FE analyses which can be a step towards standardizing IHD in composite materials to benefit the residual stress community.

1. ASTM E837-20. *Standard Test Method for Determining Residual Stresses by the Hole-Drilling Strain-Gage Method*. ASTM International, West Conshohocken, PA, www.astm.org, 2020.
2. Akbari S, Taheri-Behrooz F, and Shokrieh MM. Characterization of residual stresses in a thin-walled filament wound carbon/epoxy ring using incremental hole drilling method. *Composites Science and Technology*, **94**:8–15, 2014. ISSN 02663538. doi: <https://doi.org/10.1016/j.compscitech.2014.01.008>.
3. L. Lu, P. Jin, G. Pang, Z. Zhang, G.E. Karniadakis, Learning nonlinear operators via DeepONet based on the universal approximation theorem of operators, *Nature Machine Intelligence*. **3**:218–229, 2021. doi: <https://doi.org/10.1038/s42256-021-00302-5>.



S3 - 2

RESIDUAL STRESS MEASUREMENTS OF A NUCLEAR POWER PLANT PIPE BEFORE AND AFTER WELD REPAIRS

M. Yescas¹, B. Le Gloannec¹, S. Paddea², F. Hosseinzadeh², E. Kingston³, P. J. Bouchard²

¹Framatomeirst, 1 Place Jean Millier, La Défense, France

²Stress-Space Ltd., Atlas Building R27 Harwell Campus, Didcot, UK

³VEQTER Ltd., 8 Unicorn Business Park, Withby Road, Brislington, Bristol, UK
miguel.yescas@framatome.com

Nuclear power plant systems are constructed by joining pressure vessels and piping components using modern welding processes, however welding, and weld repairs which are sometimes necessary, introduce high magnitude residual stresses. Such stresses are significantly reduced by applying a stress relief heat treatment (SRHT) typically at temperatures close to 600°C for the carbon-manganese steel joints. This paper deals with the characterisation of weld residual stresses of a micro-alloyed carbon-manganese ferritic steel pipe with a U-groove girth weld of 40 mm thickness. Residual stress measurements were conducted at different stages; as-welded (AW) and SRHT and after different weld repair configurations. The objectives were to confirm the efficiency of the SRHT and characterise the residual stress profiles induced by the local repairs.

The residual stress measurements were conducted using different measurement techniques, namely Deep Hole Drilling (DHD) at the weld centre-line, and the multi-cut Contour method for the weld repairs. The results confirmed that the SRHT has significantly reduced the welding stresses in the girth weld, from a maximum of 500 MPa in the as-welded condition to <100 MPa in most of the pipe thickness with a peak of 150 MPa at about 10 mm from the outer diameter after SRHT. It was also found that the repair welds introduce more complex high magnitude distributions of residual stresses into the welded pipe in as-welded condition, thus, maximum tensile hoop stresses higher than the yield strength of the weld metal were measured near the repair weld centreline in the deep repairs; in the range of 550 – 650 MPa.

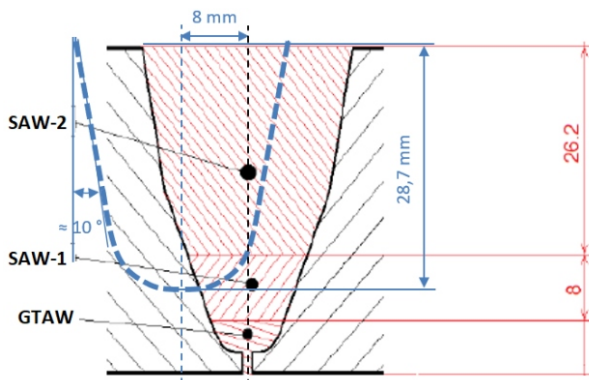


Figure 1. Schematic drawing of the original “U” groove and the repair excavation (dashed blue line).

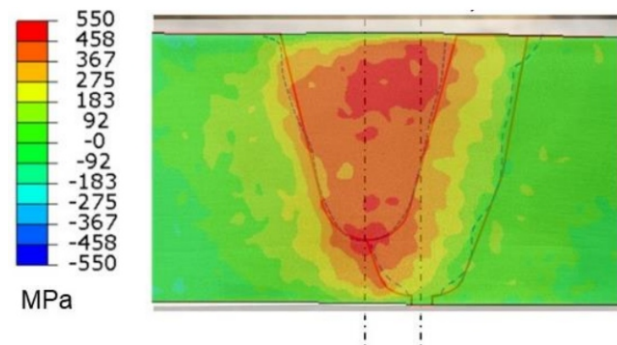


Figure 2. Residual hoop stress Contour map obtained on one of the weld repairs conducted on this project in the as-welded condition.

S3 - 3

MEASUREMENTS OF RESIDUAL STRESS IN AN INTERNATIONAL BENCHMARK SPECIMEN – NET TG8

C. E. Truman

University of Bristol, Bristol, BS8 1TR, UK
c.e.truman@bristol.ac.uk

Within the NeT project [1] Task Group 8 (TG8) examines a steel plate (French grade 18MND5, which is similar to ASTM A508 Gr.3) containing a five pass “slot” weld made with Ni base alloy (Alloy 52) consumables. NeT TG8 is motivated by welding repair issues, and is managed by EDF, France. The TG8 round robin specimen is closely based upon the TG4 design, except for the plate thickness that is increased to 30 mm for more thermal inertia, self-clamping conditions and to reduce distortions that may affect the accurate definition of residual measurement position. It thus presents all the advantages and challenges of the TG4 specimens, namely, the generation of a complex 3D residual stress distribution in a compact, portable specimen that is amenable to rapid measurement of residual stresses by diverse techniques, with a significant volume of weld metal that undergoes multiple high temperature thermo-mechanical load cycles. The use of a nickel-based alloy as filler metal adds considerable residual stress measurement challenges, while this configuration undergoes a complex mismatch behaviour with the base metal where phase transformations and tempering effects occur in the Heat Affected Zone.

This paper presents through-thickness measurements of the longitudinal, transverse and shear residual stresses present in the as-welded TG8 sample. Measurement results are obtained using the incremental deep hole drilling

(iDHD) technique [3] at weld centre and weld stop. Comparisons are made to other techniques and numerical simulations. The residual stresses are then mapped into a finite element model and used as a set of initial conditions for a simulation of the post weld heat treatment (PWHT) process. Finally, further iDHD and DHD measurements are undertaken on a post weld heat treated sample (termed “phase 2”) and compared to predictions. The results will be contributed to the international round robin. The effectiveness of the PWHT process will be considered.

1. V. Robin, J. Draup, M. C. Smith, A. Vasileiou, V. Akrivos, R. C. Wimpory, L. Depradeua, A. Brosse, D. Gallitelli, F. Hosseinzadeh, C. E. Truman, S. Pascal, S. Hendili, J. Delmas and C. Ohms, NeT Project Task Group 8 – An international benchmark on residual stress assessment for welding repair with dissimilar materials – first phase results, *Proceedings of the ASME 2023 Pressure Vessels and Piping Conference*, 2023.2. M C Smith, A C Smith, C
2. Ohms and R C Wimpory, The NeT Task Group 4 residual stress measurement and analysis round robin on a three-pass slot-welded plate specimen, *International Journal of Pressure Vessel and Piping* 164, 3-21 (2018).
3. A. H. Mahmoudi, S. Hossain, C. E. Truman, D. J. Smith and M. J. Pavier, A new procedure to measure near yield residual stresses using the deep hole drilling technique, *Experimental Mechanics*, 49, 595-604, 2009.

S3 - 4

RAILWAY AXLE: RESIDUAL STRESSES MEASUREMENTS BY THREE COMPLEMENTARY METHODS

A. Ratier¹, Y. Cheynet², P. Feraud¹

¹Agence d'Essai Ferroviaire, SNCF, Vitry-sur-Seine, France

²MDI-X, SNCF, Saint-Denis, France
Alexis.ratier@sncf.fr

For passenger's safety and to improve rolling stock maintenance, the French railway company SNCF is studying the optimization of mechanical components. As part of a project aimed at making railway axles more resistant by heat treatment, the Railway Testing Agency studied the residual stress levels reached in these axles by three complementary methods. These three methods are X-Ray Diffraction, DHD method and contour method. The XRD analyzes were carried out in our laboratory while the deep drilling

and contour methods were outsourced. The two materials of railway axles, A4T steel (25CrMo4, bainitic) and A1N steel (C40, ferritic-pearlitic), were studied. This article presents the results obtained by each of these three methods as well as their complementarity for an in-depth study of residual stresses.



S3 - 5

RESIDUAL STRESS-BASED HOLE EXPANSION PROCRS OPTIMIZATION AND INVESTIGATION OF RESIDUL STRESS EFFECT ON FATIGUE CRACK GROWTH

Min-Jae Baek¹, Dong-Jun Lee¹, Moo-Young Seok¹, Hyoen-il Park¹,
Hyun-sung Choi¹, Yong-Nam Kwon¹, Tae-Gyu Park²

¹*Aerospace Materials Center, Korea Institute of Materials Science, 797 Changwondaero, Changwon, Gyeongnam-do 51508, Republic of Korea*

²*Korea Aerospace Industries Chinhwangyeong-ro, Geumseo-myeon, Sancheong-gun, Gyeongsangnam-do, 52214 Republic of Korea*
qoralswo12@kims.re.kr

Residual stress induced plastic deformation during the fabrication of aircraft components significantly influences their fatigue life and crack propagation characteristics. Hole expansion process has been widely used to generate residual stress in these components. By expanding the hole around a designated area, this process generates compressive residual stress, effectively mitigating crack growth. The surface compressive residual stress augments the fatigue limit and enhances mechanical properties, particularly by suppressing stress corrosion cracking (SCC). Achieving the desired magnitude of residual stress necessitates the design of an optimal hole expansion process. Conducting repetitive experimental designs for this purpose proves to be prohibitively costly and time-consuming. Thus, it is necessary to efficiently analyze the relation be-

tween the process variables and the primary outputs through finite element analysis. In this study, the optimized hole expansion process has been design by analyzing the relation between design variables of hole expansion process such as Insert Angle, Mandrel Diameter, and Plate Hole Diameter and the primary outputs of the process such as residual stress magnitude and distribution, and stress of mandrel. By utilizing the resultant optimal process, we have compared and assessed the residual stress induced in the material during the hole expansion process using three different type of measurement methods, namely X-ray diffraction (XRD), hole drilling, and contour analysis. Subsequently, we have analyzed the implications of these findings on fatigue crack growth.

Session IV - Mechanical Relaxation Methods 2

S4 - 1

THE USE OF PLASMA FOCUSED ION BEAM DIGITAL IMAGE CORRELATION TO INVESTIGATE MICRO-RESIDUAL STRESSES IN FUSION REACTOR DISSIMILAR JOINTS**O. Mohamed¹, B.Zhu¹, D.England¹, Y.Wang³, J.H.You⁴, *T.Sui^{1,2}**¹*School of Mechanical Engineering Sciences, University of Surrey, Guildford, Surrey, GU2 7XH, UK*²*National Physical Laboratory, Hampton Road, Teddington, TW11 0LW, UK*³*United Kingdom Atomic Energy Authority, Culham Centre for Fusion Energy, Culham Science Centre, Abingdon, Oxon, OX14 3DB, UK*⁴*Max Planck Institute for Plasma Physics, Boltzmann Str. 2, 85748, Garching, Germany
t.sui@surrey.ac.uk*

The prospect of fusion energy is an exciting endeavour for humanity, able to provide an abundant and greenhouse gases free form of energy that will be undoubtedly play a future pivotal role in decarbonisation and tackling climate change worldwide [1]. Hence, it is of no surprise that advancements in fusion research have been accelerating through global projects such as the International Thermonuclear Experimental Reactor (ITER) and its successor, DEMONstration Power Plant (DEMO), aimed at proving the feasibility of fusion on a commercial level. The assessment of structural materials is vital to ensuring the safety, reliability, and longevity of fusion reactors. These materials encounter numerous challenges stemming from the unique fusion environment, where they are subjected to high heat fluxes, irradiation, and plasma bombardments. Such extreme conditions can inevitably impact the properties and microstructures of the materials. Furthermore, the joining of dissimilar materials is necessary from a design perspective in many reactor components [2]. This is bound to induce residual stresses, which can further degrade and reduce the service life of components [3].

The combination of Plasma Focused Ion Beam and Digital Image Correlation (PFIB-DIC) creates a powerful tool that enables the analysis of multiscale residual stress states [4]. Particularly, type II residual stresses which are typically ignored despite their influence on the initiation and propagation of microcracking [5]. The principles of measuring the micro residual stresses using FIB-DIC rely on utilising ions to mill micro-trenches in the material, while subsequently using Scanning Electron Microscopy (SEM) to image the milling process. DIC analysis is then applied to the relevant regions of SEM images to extract the displacement and strain fields, from which the residual stresses can be accurately determined [6]. In this paper, the use of PFIB-DIC technique to assess the residual stresses in Tungsten (W)/Copper (Cu)/ Copper Chromium Zirconium (CuCrZr) dissimilar joints used in the critical divertor component is presented. The effects of HHF (20 W/m²) on the W armour microstructure and residual stress profile is also evaluated. It was found that the distribution of micro-resid-

ual stresses near the interface was primarily influenced by the texture and polycrystalline grain structure of W and CuCrZr. The larger grains in the pure Cu layer allow stress mapping over a single grain. The results reveal heightened compressive residual stresses near the Cu/W interface, as expected due to the notable difference in the coefficient of thermal expansion between Cu and W. HHF were also found to affect the hardness and residual stress distribution across W, this was attributed to the recrystallisation that occurs which influences the dislocation density, confirmed by Electron Back Scatter Data (EBSD). The findings will provide a better understanding of residual stress generation within the Divertor component of fusion reactors.

1. F. Romanelli, L. H. Federici, R. Neu, D. Stork, and H. Zohm, "A roadmap to the realization of fusion energy," *Proc. IEEE 25th Symp. Fusion Eng.*, pp. 1–4, Jan. 2013.
2. J. H. You *et al.*, "Conceptual design studies for the European DEMO divertor: Rationale and first results," *Fusion Engineering and Design*, vol. 109–111, no. PartB, pp. 1598–1603, Nov. 2016, doi: 10.1016/J.FUSENGDES.2015.11.012.
3. H. E. Coules and G. C. M. Horne, "Effects of residual stresses and localised strain-hardening on the fracture of ductile materials," *Procedia Structural Integrity*, vol. 17, pp. 934–941, 2019, doi: 10.1016/J.PROSTR.2019.08.124.
4. B. Zhu *et al.*, "A novel pathway for multiscale high-resolution time-resolved residual stress evaluation of laser-welded Eurofer97," *Sci Adv*, vol. 8, no. 7, Feb. 2022, doi: 10.1126/sciadv.abl4592.
5. H. Fu *et al.*, "Evolution of the residual stresses of types I, II, and III of duplex stainless steel during cyclic loading in high and very high cycle fatigue regimes," *Int J Fatigue*, vol. 142, p. 105972, Jan. 2021, doi: 10.1016/J.IJFATIGUE.2020.105972.
6. E. Salvati and A. M. Korsunsky, "An analysis of macro- and micro-scale residual stresses of Type I, II and III using FIB-DIC micro-ring-core milling and crystal plasticity FE modelling," *Int J Plast*, vol. 98, pp. 123–138, Nov. 2017, doi: 10.1016/j.ijplas.2017.07.004.



S4 - 2

RESIDUAL STRESS ANALYSIS IN AN ADDITIVE MANUFACTURED HIGH-STRENGTH STEEL COMPONENT USING THE CONTOUR METHOD

G.A. Shabdali¹, K. Wandtke¹, A. Kromm¹, D. Schroepper¹, T. Kannengiesser¹,
R. Scharf-Wildenhain², A. Haelsig², J. Hensel²

¹ Bundesanstalt für Materialforschung und -prüfung, BAM, 12205 Berlin

² Technische Universität Chemnitz, Professur Schweißtechnik, 09126 Chemnitz
karsten.wandtke@bam.de

Additive manufacturing processes such as direct energy deposition (DED) arc welding enable the weight-optimized and near-net-shape production of complex structures. Lightweight construction principles allow a reduction of CO₂ emissions by saving time, costs, and resources. Further efficiency can be achieved by using high-strength steels. Filler metals are already available on the market, but a lack of knowledge and guidelines regarding welding residual stresses during production and operation prevents a

wide industrial application. This study focuses on the investigation of residual stresses using the contour method. This method enables the analysis of the two-dimensional map of residual stresses normal to a cutting plane using a finite element model. Complementary X-ray diffraction confirmed high tensile residual stresses in bulk and surface of the structure. Hardness measurements indicate a correlation between the local microstructure and the residual stress formation.

S4 - 3

SENSITIVITY ANALYSIS OF THE CONTOUR METHOD: INFLUENCE FROM MEASURING AND PROCESSING OF THE DEFORMATION DATA

Jonas Holmberg¹, Johan Berglund¹, Hue Houg² Peter Ottosson¹, Ramin Moshfegh,
Mats Werke¹

¹RISE Research Institutes of Sweden AB, Argongatan 30, 431 53 Mölndal, Sweden

²System 3R International AB, Sorterargatan 1, 162 50 Vällingby, Sweden
jonas.holmberg@ri.se

Knowing the internal stress state of materials and components is often of great interest as it may lead to distortion during a subsequent material processing, such as machining the final geometry of a part. This is especially critical and may result in severe distortion if the internal stresses are high and unevenly distributed as the final geometry is slender. Much work has been done to develop of the contour method, including useful guidelines [1, 2], which guide the user through the basic processing steps of; (1) Stress free sectioning, (2) high-resolution surface geometry measurement of sectioned surfaces (3) data analysis of the deformed surfaces and reconstruction of stresses by FEA. However, the impact and sensitivity of the recommended processing steps is not well described, which has been the intention in this work.

Investigations have been performed on a tool steel, modified AISI 420, starting with contour measurement of the residual stresses from material manufacturing, which

was followed by measurement after heat treatment for the same material. Evaluation of the impact on the final calculated stresses has been done by using different measurement systems, an optical 3D scanner as well as probe measurements using a Coordinate Measuring Machine (CMM), for acquiring the high-resolution geometry of the cut surface. The impact from processing the data was also evaluated for the calculated stresses by altering the cut-off length of the applied filter when acquiring the mean deformation surface. The objective has been to study the robustness of the contour method in this perspective.

- Hosseinzadeh F, Kowal J, Bouchard PJ (2014) Towards good practice guidelines for the contour method of residual stress measurement. The Journal of Engineering 2014:453–468. <https://doi.org/10.1049/joe.2014.0134>
- Prime MB, DeWald AT (2013) The Contour Method. In: Practical Residual Stress Measurement Methods. pp 109–138.

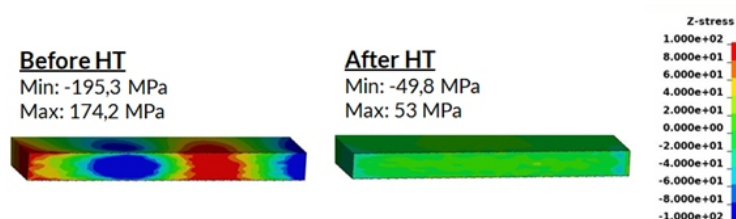


Figure 1. Example of contour stress measurements of AISI 420 steel plates before and after heat treatment.

S4 - 4

AN ALGORITHM FOR CORRECTING THE ZERO-DEPTH ERROR IN HOLE-DRILLING MEASUREMENTS

A. Benincasa¹, M. Beghini², T. Grossi², C. Santus²

¹SINT Technology Srl, Florence, Italy

²Dipartimento di Ingegneria Civile e Industriale, Università di Pisa, Italy
tommaso.grossi@ing.unipi.it

Errors encountered in hole-drilling residual stress measurements are commonly classified as “left-side” and “right-side” errors [1], contingent upon whether they primarily impact the calibration matrix or the strain readings, respectively. Left-side errors predominantly originate from factors such as inaccuracies in hole eccentricity and depth, whereas right-side errors typically result from sources like electrical noise and residual stresses induced by drilling. Among left-side errors, the uncertainty associated with zero-depth detection plays a pivotal role in determining the accuracy of residual stress values at the surface [2], a domain where X-ray diffraction measurements are conventionally perceived to possess an advantage over hole-drilling methods.

This study introduces a corrective algorithm designed to address inaccuracies in zero-depth detection, validated through experimental comparisons with externally applied stress distributions. These comparisons are facilitated by a calibration bench developed by the authors [3-5], enabling the application of a known bending stress distribution on a specimen while simultaneously conducting X-ray diffraction or hole-drilling residual stress measurements. Therefore, a direct validation of residual stress results is achieved, up to the accuracy of the applied bending stresses, which surpasses that of the identified residual stresses by at least an order of magnitude.

Through a comparative analysis of surface residual stresses obtained via hole-drilling measurements comple-

mented with the proposed correction algorithm and those obtained with standard X-ray diffraction measurements, it is demonstrated that, when the zero-depth error is appropriately accounted for, the accuracy of the two methods at the surface is clearly comparable.

1. G. S. Schajer and E. Altus, "Stress Calculation Error Analysis for Incremental Hole-Drilling Residual Stress Measurements," *J. Eng. Mater. Technol.*, vol. **118**, no. 1, pp. 120-126, Jan. 1996, doi: 10.1115/1.2805924.
2. D. Peral, J. de Vicente, J. A. Porro, and J. L. Ocaña, "Uncertainty analysis for non-uniform residual stresses determined by the hole drilling strain gauge method," *Measurement*, vol. 97, pp. 51-63, Feb. 2017, doi: 10.1016/j.measurement.2016.11.010.
3. M. Beghini, T. Grossi, C. Santus, and E. Valentini, "A calibration bench to validate systematic error compensation strategies in hole drilling measurements," in ICRES 11-11th International Conference on Residual Stresses, 2022.
4. M. Beghini, T. Grossi, C. Santus, and E. Valentini, "Revealing systematic errors in hole drilling measurements through a calibration bench: the case of zero-depth data," *J. Theor. Comput. Appl. Mech.*, Oct. 2023, doi: 10.46298/jtcam.10080.
5. M. Beghini, T. Grossi, and C. Santus, "Validation of a strain gauge rosette setup on a cantilever specimen: Application to a calibration bench for residual stresses," *Mater. Today Proc.*, p. S2214785323031371, Jun. 2023, doi: 10.1016/j.matpr.2023.05.505.

S4 - 5

MAPPING RESIDUAL STRESSES IN NON-CONDUCTIVE MATERIALS USING THE CONTOUR METHOD

Neil Hollyhoke¹, Daniel Holman², Jeferson Araujo de Oliveira¹

¹The Open University, United Kingdom

²Magma Global Ltd. United Kingdom
neil.hollyhoke@open.ac.uk

Residual stresses are a key to understanding how the manufacturing processes influence the structural integrity of safety-critical mechanical components. There are several residual stress measurement techniques available, among which, the contour method stands out as capable of generating a cross-sectional map of the residual stresses after introducing a cut into the test component of interest. This cut has a very particular set of requirements, such as: already cut surfaces cannot be re-cut and the cut width needs to be

uniform throughout. Because of these stringent requirements, to date, only electro-discharge machining (EDM) has been successfully used to map residual stresses across a test sample. Attempts to use other techniques, such as waterjet or laser cutting have failed to produce cut surfaces with high enough quality. Since Electro-discharge machining can only be used to cut electrically conductive materials, the contour method has been limited to this type of material.



For the first time, we present the results from the use of abrasive diamond wire cutting for *measuring a non-conductive PEEK pipe using the contour method*. Results show the expected trend and magnitudes in the hoop stresses and also variations in the residual stresses where the manufacturing process had a discontinuity. These are

encouraging preliminary results and the cutting method will be explored further for the application of the contour method in materials that were previously impossible.

S4 - 6

THE USE OF NON-STANDARD TRIAXIAL STRAIN GAUGE ROSETTES FOR INCREMENTAL HOLE-DRILLING IN COMPOSITE LAMINATES

R.G. Reid, T.C. Smit

School of Mechanical, Industrial and Aeronautical Engineering, University of the Witwatersrand, Private Bag 3, Wits 2050, South Africa
Robert.Reid@wits.ac.za

Fibre reinforced plastic (FRP) laminates are not crystalline and hence residual stress measurement in these materials requires the use of relaxation techniques. Amongst the range of techniques available, incremental hole-drilling (IHD) is widely used and accepted. A standardized test procedure (ASTM E837 [1]) exists for IHD in isotropic materials, which includes the use of specific strain gauge rosettes for particular hole diameter ranges. While the standardized test procedure does not extend to composite materials, the general procedure is the same and the special strain gauge rosettes developed for IHD are still used. Numerous manufacturers provide these special hole-drilling rosettes, however in recent years the 350 variants of these rosettes have been discontinued. As a result, it is currently necessary to use the 120 hole-drilling variants of these rosettes.

This poses problems in FRP laminates because they have poor thermal conductivity and the heat generated by current flowing through the strain gauge grid is not easily dissipated. This can lead to localized heating of the gauge area, even extending to the location where the hole is to be drilled and artificially introducing additional residual stresses beyond those that are under investigation. This effect can cause significant errors in the measured strains and hence the calculated stress distributions. The most effective way of reducing this issue is to reduce the excitation voltage of the grids in the rosette, but this reduces the sensi-

tivity of the strain measurements. Depending on the situation, this loss of resolution can significantly impact on the accuracy of the residual stress measurements.

Since IHD in FRP laminates can never conform to the ASTM E837 standard due to the orthotropic nature of each ply in the laminate, it is possible to exploit the opportunities available in deviating from the standard. One possible approach is to revert to the non-standard 350 strain gauge rosettes that are widely available, but which are not intended for IHD. This approach allows the use of a higher excitation voltage with a corresponding increase in sensitivity without significant self-heating effects. The disadvantage of this approach is that the non-standard rosette configurations are not optimized for use with IHD. There thus exists the possibility of a loss in resolution, and an increase in hole positioning (offset) errors, depending on the location and size of the drilled hole within the rosette.

The position and size of the hole relative to a non-standard triaxial rosette is therefore of particular importance and the optimal position needs to be determined to ensure that these effects do not negate the increase in sensitivity associated with a higher excitation voltage. The optimal position probably varies depending on the nature of the residual stresses present. For instance, in a biaxial laminate, where it is expected that the residual shear stresses are negligible, it is possibly best to optimize the position and size of the hole such that the 0° and 90° grids have maximum

Table 1. Sources of uncertainty and their assigned probability density functions.

x_i	Description	$p(x_i)$	Type	Nominal value, uncertainty
$meas$	Measured experimental strain	Normal	B	Indicated strain, 1.54 %
x_{offset}	Hole offset in the x direction	Rectangular	B	0 m, 5 m
y_{offset}	Hole offset in the y direction	Rectangular	B	0 m, 5 m
noise	Experimental noise (350)	Normal	A	0, 0.61 m/m
noise	Experimental noise (120)	Normal	A	0, 1.36 m/m
FE	Finite element calculations	Normal	B	FE output, 2 %

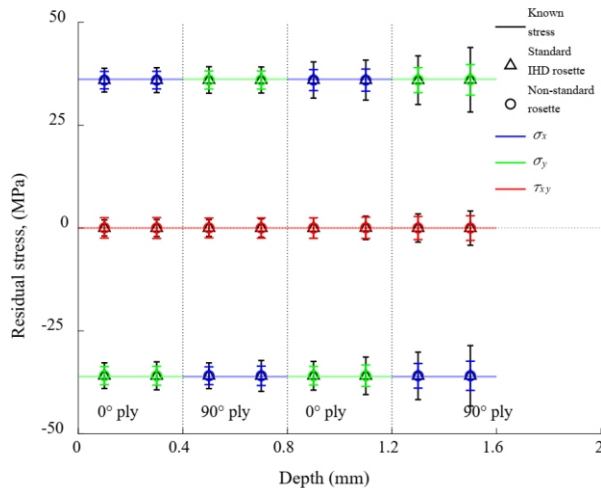


Figure 1. Measured residual stress distribution in a $[0^\circ/90^\circ/0^\circ/90^\circ]_s$ laminate.

sensitivity. In contrast, where it is expected that significant shear stresses are present, a compromise is required so that all three grids provide acceptable sensitivity, without any single one of them being optimized. In such a situation, the hole must move closer to the 45° grid, and is no longer located on the axes of either of the remaining grids. In consequence, there can be significant transverse strains across these grids. The calibration coefficients therefore need to be carefully calculated making use of finite element models that properly represent the tested geometry. Since this approach is required even when using special IHD gauges, however, this is not a significant disadvantage of the proposed method.

This work investigates the use of the readily available KFRPB-2-350-D22 strain gauge rosette from Kyowa [2]. This rosette has gauges of 350 W resistance and 2 mm length with grids aligned at 0° , 90° and 45° . The 45° grid of this rosette is located further from the intersection of the axes of the 0° and 90° grids than these two other grids. Two symmetric GFRP laminates of eight plies each; $[0^\circ/90^\circ/0^\circ/90^\circ]_s$ and $[+45^\circ/-45^\circ/0^\circ/90^\circ]_s$, respectively, are investigated by simulating the IHD process conducted on known stress distributions with holes of 4 mm diameter. The hole of the first laminate is located at the intersection

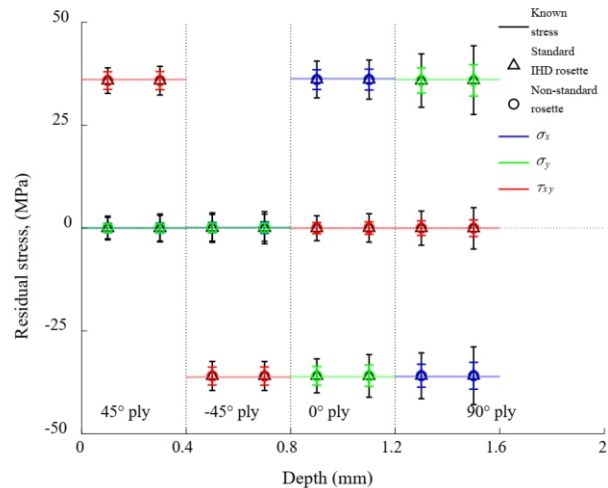


Figure 2. Measured residual stress distribution in a $[+45^\circ/-45^\circ/0^\circ/90^\circ]_s$ laminate.

of the 0° and 90° grids. The hole of the second laminate is located at an optimised position closer to the 45° gauge along its axis and is consequently offset from the axes of the other grids. Results are compared to those resulting from the use of standard IHD rosettes of 120 W resistance, KFGS-3-120-D28 [2]. The dominant experimental uncertainty sources used in the simulations are shown in Table 1.

Figs 1 and 2 show that the non-standard KFRPB-2-350-D22 strain gauge rosette provides accurate residual stress measurements for both laminate configurations considered, and with reduced uncertainty. The reduction in stress uncertainty is a result of the reduced experimental strain noise of the 350 gauges arising from their higher excitation voltage. The RMS of the stress uncertainty over the entire measurement depth is reduced by roughly 50 % compared to the standard KFGS-3-120-D28 IHD rosette.

1. ASTM E837-20. *Standard Test Method for Determining Residual Stresses by the Hole-Drilling Strain-Gage Method*. ASTM International, West Conshohocken, PA, www.astm.org, 2020.
2. Kyowa Electronic Instruments Co, Ltd. *General Catalogue 2022*, <https://kyowa-ei.meclib.jp/e2022/book>.